Network topology and evolution of the gene co-expression of T-cells during immuno-senescence

Megan L. Mair[1] ¶, Nicolas Tchitcheck, Tarynn M. Witten[*¶2], Véronique Thomas-Vaslin[3]

[1] Virginia Commonwealth University, Center for the Study of Biological Complexity

[2] Department of Computer Science

US-VA 23284-2030 Richmond, United States

[3] Sorbonne Université, INSERM, Immunology, Immunopathology, Immunotherapies, UMRS959, F-75013 Paris, France

* Corresponding Author Address: Prof. Tarynn M. Witten, Dept. of Computer Science, Room E4225, College of Engineering, Virginia Commonwealth University, Richmond, VA 23284-3019.

Corresponding Author Email: tmwitten@vcu.edu

¶ These authors contributed equally to this work

Abstract

To better understand the potential impact of the gene expression network structure on the dynamics of immune-senescence and defects of cell functions during aging, we investigated network structures in both young and old individuals. We analyzed the gene co-expression networks (GCNs) derived from an aging signature of 130 immune-related genes obtained from CD3+ T-cell splenocytes extracted from FVB/N, C57BL/6N, and BALB/c mice at ages 2 and 22-24 months. The network structure for the two different mouse age-groups was derived and subsequently analyzed. Analysis of network hubs using clustering coefficients, degree, betweenness, eigenvector, and closeness centralities, as well as local, indirect, and total influence measures, demonstrated changes in gene behavior and network control between the two age groups. Our quantification shows that the young, 2-month old mouse network is more organized than the 22-24-month, old mouse network, while the network structure of the older mouse GCN appears to be far more complicated but far more dispersed. Changes in network structure between the old and young mice suggest deterioration in transcription regulation with age in peripheral T-cells, particularly within the TCR signaling pathway, and potential compensatory mechanisms in older T-cells to overcome loss to regular function resulting from transcriptional irregularity. These results demonstrate the need for more research into gene co-expression in peripheral T-cells in order to better understand both network irregularities and the phenotypic dysfunction observed in older individuals.

Author Summary

In order to better understand the potential mechanisms of transcriptional irregularities in the immune system with aging, we analyzed the structure of gene co-expression networks of T-cells extracted from the spleens of 2 and 22-24-month old mice. Gene co-expression describes the correlation relationship between two expressed genes; as the expression of one gene goes up, the expression of another gene might also increase (or, conversely, decrease). Strong gene co-expression relationships can signal the existence of a number of important biological phenomena, such as two genes belonging to a transcription pathway or protein structure. Network diagrams visualizing these co-expression relationships in both younger and older mice demonstrated the existence of differences in network structure and properties that may be attributed to the aging of the immune system. Network mathematical methods were used to examine the complexity of each network. We found that the younger mouse network was more organized than the older mouse network. The older mouse group exhibited a 255% increase in co-expression relationships but a decrease of 92% of the connections from the young mouse network. This suggests the older mouse T-cells suffer dysfunction at a transcriptional level. This results in the loss of regular immune and cellular functions. These results demonstrate the importance of future research into gene co-expression to decipher senescence or diseases that perturb gene expression through time.

Introduction

Aging is a natural process that progressively alters biological cell functions at the microscopic level with cell senescence, and extends up to the organ level and overall function of the organism, leading to complex disorganization at various scales in living systems [1]. The network connectivity between the nodes composing the multi-level hierarchical network of

64 "aging" could thus be altered at various biological levels. This could lead to rupture of stability
65 and robustness of dynamic interweaved networks with age.

66 At the mesoscopic level, the population of individuals aged 65 and over is increasing [2].
67 The economic and biomedical influence of the elderly population will have a significant impact
68 upon the global economy [3-5]. Chronic inflammation and susceptibility to infection are traits of
69 immuno-senescence, the term used to describe the overall age-related changes of the immune
70 system [6-10]. Immune dysfunction in the elderly contributes to increased susceptibility to
71 infection and inflammation [11-13]. Immuno-senescence can have a negative impact on health
72 outcomes including morbidity and mortality in older adults [6, 10-18]. This was recently
73 underlined with the Covid-19 pandemic, where older individual were more susceptible to severe
74 disease and mortality [19].

75 Aging is often characterized by perturbations and/or remodeling of the T-lymphocyte
76 system [20-23]. Aging contributes to the decrease of naïve T-cell production [24], first by thymic
77 involution starting at puberty. These perturbations of production are then compensated by
78 increasing the selection and the proliferation of effector/memory T lymphocytes populations,
79 which were previously exposed to an antigen. As the organism ages, the accumulated
80 effector/memory cells often become senescent non–functional T-cells. These fill the
81 "immunological space," replacing the decreasing population diversity of naïve cells, which are
82 able to recognize and combat sources of new antigens.

83 Immuno-senescence also affects mice; mice are thus a good model to study the dynamics
84 of T lymphocyte aging through micro (cells) and macro (tissues/organs) levels. Mice have
85 previously been used to demonstrate other changes in T lymphocyte biology in the context of
86 aging. For example, partial clonal deletion is known to occur in the spleen in old mice. Previously,

Thomas-Vaslin *et al*. quantified the heterogeneity of T-cell population proportions based on their proliferation rates, according to various mice genetic origins [25]. This revealed decreased proliferative and renewal capacities of T-cells with aging. These selection processes also result in a diminished T-cell receptor (TCR) repertoire biodiversity, required for the recognition of new antigens [23]. Thomas-Vaslin *et al*. have additionally demonstrated that T-cell homeostasis is maintained in young mice after a transient perturbation [26], with a biodiversified repertoire. However, at mid-life the immuno-senescence decreases the turnover and proliferation of naive T-cells with new TCRs, while memory T-cells and oligoclonal expansion accumulates. The consequences of the natural immunodepression during aging could be exacerbated by the effects of transient perturbations such as immunosuppressive treatments which kill dividing cells, like chemotherapy [25]. Most immunopathologies in humans also drive oligoclonal expansions of T-cells [27].

These observations suggest that the T-cell dynamic network interactions and regulation processes could be influenced by age. Our hypothesis is that responses to molecular perturbations, from the level of gene transcription, is optimized in the T-cells of young mice, and that this robust response is diminished in old mice.

Understanding the complexity of gene expression and cell pathways can be approached through the analysis of network gene co-expression relationships [28]. Gene co-expression networks have been used to study the biology of organisms such as plants, mice, and humans [29-31]. Gene co-expression describes simple correlation relationships between the expression levels of two genes. For example, as the expression of one gene increases, a given gene might have a strong positive or negative correlation with the expression of a second gene. Strong gene co-expression relationships correlate with a number of intracellular biological processes, including

transcription pathways, protein complex formation and cell signaling. Changes in co-expression relationships and subsequent network topology can therefore provide insight into altered biological pathways, for instance, in the contexts of disease or aging [28, 32-33]. Gene co-expression analysis through network structures can begin to provide a more holistic view of biological processes related to gene expression, allowing for the detection of changes not otherwise evident in simple gene expression data.

In order to understand these more complicated interactions, mathematical, bioinformatics and computational methods may be brought to bear. Among the system-level tools in these fields are those of network analysis. There are already a number of historical research papers that have applied network analysis techniques to studying various aging processes and variation of connectivity during aging of various species [34-45], up to the theory of aging networks. Network comparison techniques allow for the detection of potential differences in gene co-expression across a variety of biological conditions, including possible age-related changes in gene co-expression.

In this paper, we present an analysis of aging-related, dynamical transcription modification using gene co-expression data derived from peripheral T-cells from both young (2 months old) and old mice (22/24-months old). These gene co-expression networks were derived from a shared signature of 130 immune-related genes obtained from CD3+ splenocytes extracted from mice strains that display genetic variability (FVB/N, C57BL/6N, and BALB/c) [46]. We applied a number of network analysis methods to determine the existence of optimal network capacities and connectivity in young mice. We then investigated the age-related changes in network properties and structures by analyzing the loss of gene co-expression and the newly gained gene co-expression relationships in the older mouse network. We discuss how these changes may be

associated with mouse species immuno-senescence, and how these changes might give insights into the aging of the human immune system.

Results

General terminology of structure of gene co-expression networks

We investigate here the topology and evolution of gene co-expression networks (GCN), across young and old mice, tracking the lost and gained gene co-expressions and the resulting remodeling of the structure of the networks that could influence the possible robustness/efficacy/resilience of the adaptive immune cells. For the purposes of our upcoming discussion, a node/vertex/hub means a gene that is expressed as an mRNA and an edge means that there is a single link, undirected, between two expressed genes in the network (*i.e.*, there exists a strong correlation between the expression of the two linked genes). A reference for important network terminology can be found in Table 1, and important concepts are illustrated in Fig 1.

145 **Table 1. Table of network terminology.**

Term	Definition for gene co-expression network (GCN)
Node/Vertex/Hub	Gene that is expressed as an mRNA represented in the network
Edge	A link, undirected, between two expressed genes in the network, indicating a co-expression relationship between the mRNA
Degree centrality	Centrality measure denoted by the number of edges directly attached to a node
Eigenvector centrality	Measure of influence of a given node in a network. A higher eigenvector centrality score means a node is connected to many other nodes with eigenvector centrality scores
Closeness centrality	Measure of how close an individual node is to other nodes in the network
Betweenness centrality	Measure of control a node has over a network based on how a node connects and stands between other nodes
Eccentricity	The maximum distance between a node and all other nodes
Stress	The number of shortest paths passing through a given node, indicates the importance of a node holding together a network
Weiner index	Sum of all the shortest paths in the network
Local influence	The influence a node has over its directly connected, one-hop neighbors
Indirect influence	The influence a node has on its two-hop neighbors
Total influence	Weighted sum of direct and indirect influence
Clustering coefficient	Measure of degree to which nodes cluster around a given node in the network

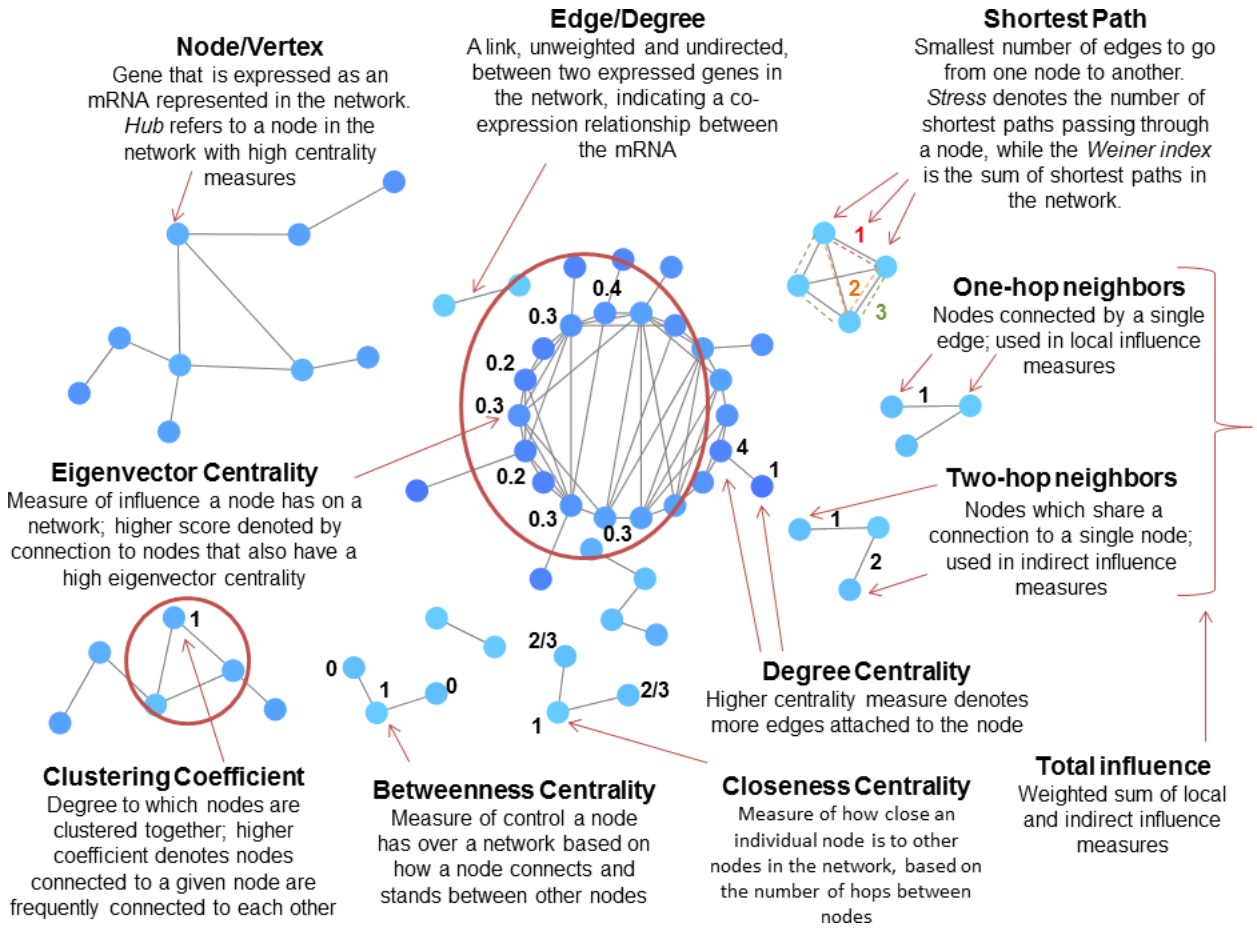

Figure 1. Diagram illustrative of key network terminology. Terminology used in this paper is important for the discussion of Gene Co-expression Networks (GCNs).

Aging signature and hierarchical clustering of mice according to gene expression in splenic T-cells.

To decipher gene expression modifications across aging, we performed a transcriptomic profiling of $CD3^+$ purified splenocytes from 12 young mice age 2 months and from 11 old mice ages 22-24 months. The ICA/GSEA method was used to identify a signature of 130 genes able to distinguish young from old mice. Interestingly, the age-related gene signature allows us to

156 segregate the 3 mice strains, considering only the young mice. However, this signature cannot
157 separate the mice according to the genetic origin of old individuals due to the high variation of
158 gene expression (S1 Figure). This suggests a precise synchronization and organization of gene
159 expression in development that could vary according to genetic origins, allowing for the optimal
160 functionality of T-cells in young mice. However, a disorganization of gene expression appears in
161 old mice that could no longer maintain their individual genetic signature. This suggests an
162 introduction of stochastic events in gene expression. To verify this hypothesis, we then proposed
163 topological analysis of the gene-co-expression network.

164 **General Network Structure of T-cell expression in the spleen of young and old mice**

165 To further understand the aging alterations that could impact T-cell functionality based on
166 our gene signature, we generated two gene co-expression networks (GCN) based on the young and
167 old aged mice. The network of young mice represent the optimal activity and functionality of the
168 pool of all splenic T-cells, based on a consensus of expression data. The network of old mice
169 represent the resilient T-cells that continue to live in the old mice, while the natural
170 immunodepression has already removed more than 80% of naïve T-cells while favoring the
171 proliferation and accumulation of effector/memory T-cells in the spleen [24-25]. Based on these
172 two networks, we performed topological analyses to compare their structures and functionalities.
173 We used various centrality network measurements applied to each GCN.

174 We first analyzed the structure of the gene co-expression network in young mice and
175 compared it to the network structure of GCN belonging to old mice. Genes expression was detected
176 with probes that cover messenger RNA from different genetic regions, including multiple probes
177 that detect particular TCR proteins encoded from stochastic gene rearrangements of VDJ genes.
178 The mRNA represented by each node is expected to give rise to the functional protein interactions

related to known intracellular pathways expressed in the sampled T-cells. S1 Table lists all of the gene transcripts found in both of the networks, along with known human orthologs and known gene functions. Network files featuring the genes that appear in each network, as well as their corresponding co-expression relationships, can be found in S2 Table (young mouse GCN) and S3 Table (old mouse GCN).

Pathway Analysis: KEGG /REACTOME

Genes appearing in the young and old mouse network were enriched in several immune system-related pathways; of the network genes contained in MSigDB, 33% in the young mouse network and 21% in the old mouse network were enriched for the REACTOME Immune System pathway. Despite having fewer nodes total, a higher percentage of genes in the young mouse network were enriched in KEGG and REACTOME immune system-related pathways compared to the older mouse network. Pathways unique to the young mouse GCN were genes involved in the translocation of ZAP-70 and the phosphorylization of CD3 and TCR zeta chains, which was significant at the 0.05 level. The old mouse GCN, on the other hand, had genes enriched for aldosterone-regulated sodium reabsorption and primary immunodeficiency, while the young mouse network did not. A complete summary of pathway enrichment results can be found in Fig 2.

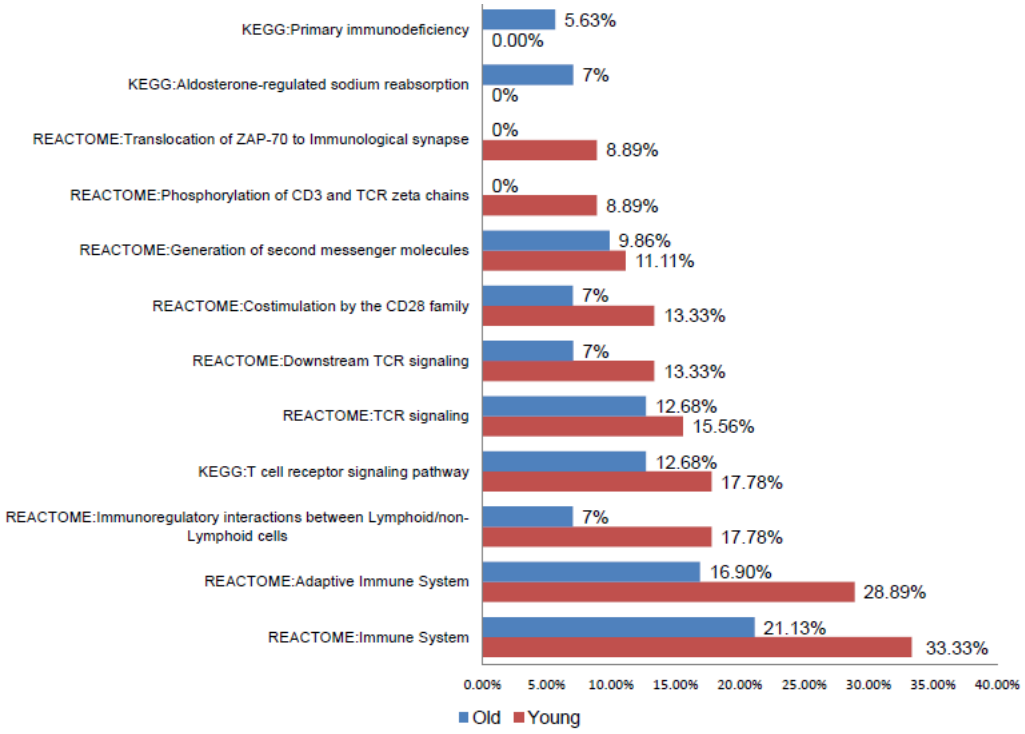

Fig 2. KEGG and REACTOME Pathway Enrichment. Percentage of genes enriched in each pathway in the young (red) and old (blue) mouse GCNs. Only the difference between the proportion of genes in the old and young networks enriched for involvement in the translocation of ZAP-70 and the phosphorylation of CD3 and TCR zeta chains was significant at the 0.05 level.

Structure of the network in young and old mice as number of nodes and edges

The range of edges per node for the younger mouse GCN was 1-10 edges, with a mean edge count of 2.656. For the older mouse GCN, the range of edges per node was 1-15 edges per node with a mean degree count of 5.922 edges per node. For the 2-month old mouse GCN, the average node degree count falls within the range typical of a biological network [47]. This is not true for the 22/24-month old mouse network. A summary of some of these network differences

208 can be found in Table 2. A t-test demonstrated a statistically significant difference between the
209 mean edge counts of the two age-groups ($p < 0.001$).

210 **Table 2: Summary of basic network statistics for the 2 and 22-24 month-old networks.**

Gene centrality measure	2-month GCN	22-24-month GCN	Difference
Mean Edge Count	2.66	5.92	Significantly different $p < 0.001$
Mean Shortest Path	2.05	3.39	Significantly different $p < 0.001$
Mean Clustering Coefficient	0.25	0.34	Significantly different $p < 0.05$
Weiner Index	2206	76617	N/A
Network Diameter	7	12	N/A
Core Network Radius	4	6	N/A

211

212 Network attributes were highly altered across the two age-related networks. The 2-month
213 GCN had a total of 64 nodes with 78 unique edges, while the 22/24-month old GCN had 102
214 nodes with 295 unique edges. A total of 53 nodes were found to be identical in both the 2-month
215 and 22/24-month old networks. What is interesting is that despite this conservation of 53 nodes,
216 only 7 edges are conserved across both networks. Table 3 lists the genes at the ends of each of
217 the 7 edges. We highlighted these conserved edges in Fig 3. As we will later describe, the 7
218 highlighted conserved pairs in Fig 3 are ranked first or second in nearly all of the network

219 centrality measures. Notably, most of the genes co-expressed and conserved between T-cells from
220 young and old mice concern the TCR, which is required to receive signals from antigens and
221 transduce signaling pathways to trigger various T-cell functions. However, the co-stimulation of
222 the TCR involving CD28 and its downstream signaling [48] is disconnected from the core
223 network gene expression in old mice, suggesting default of co-stimulation as in hallmark of
224 senescent CD8 T-cells [49]. The overall network structure for both age-groups is summarized in
225 an adjacency matrix in Fig 4.

226 **Table 3: List of the edges conserved between the young and old networks along with the**
227 **genes (nodes) that the edges connect.**

Edge number	Edges Conserved Across Networks
1	Sema4f – LOC630408
2	LOC386545 – Leprotl1
3	Pik3r1 – Dgka
4	LOC100043969 – Cd28
5	Tcrb-V8.2 – LOC100041103
6	Tes – Lat
7	Xlr4c – LOC100046087

228

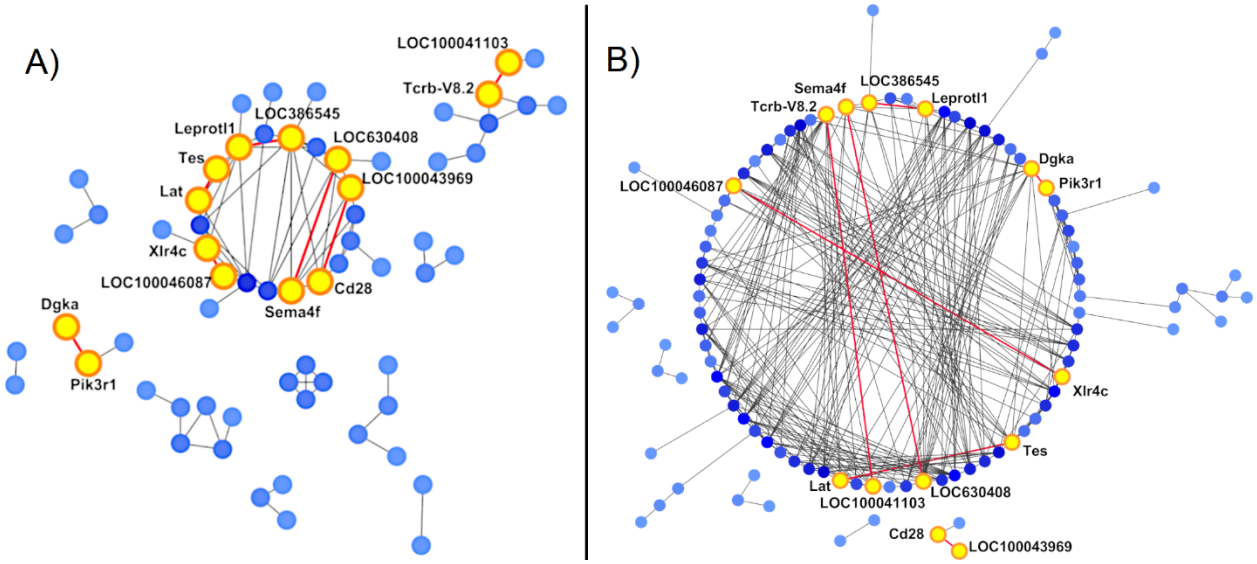

Fig 3. Network diagrams of gene co-expression with conserved edges between young and old splenic T-cells. The Spearman rank correlation reveals the gene co-expression network according to age. Darker colored nodes correspond with a higher number of edges per node (up to 10 edges in the younger mouse network and 15 edges in the older mouse network). A) The GCN constructed based upon gene co-expression in CD3+ splenocytes from 2-month old mice (64 nodes and 85 edges). B) The GCN constructed based on the old mouse data (102 nodes and 302 edges). The seven conserved edges between young (A) and old (B) mice are illustrated with the red lines. Node pairs at the ends of these edges are labeled and highlighted.

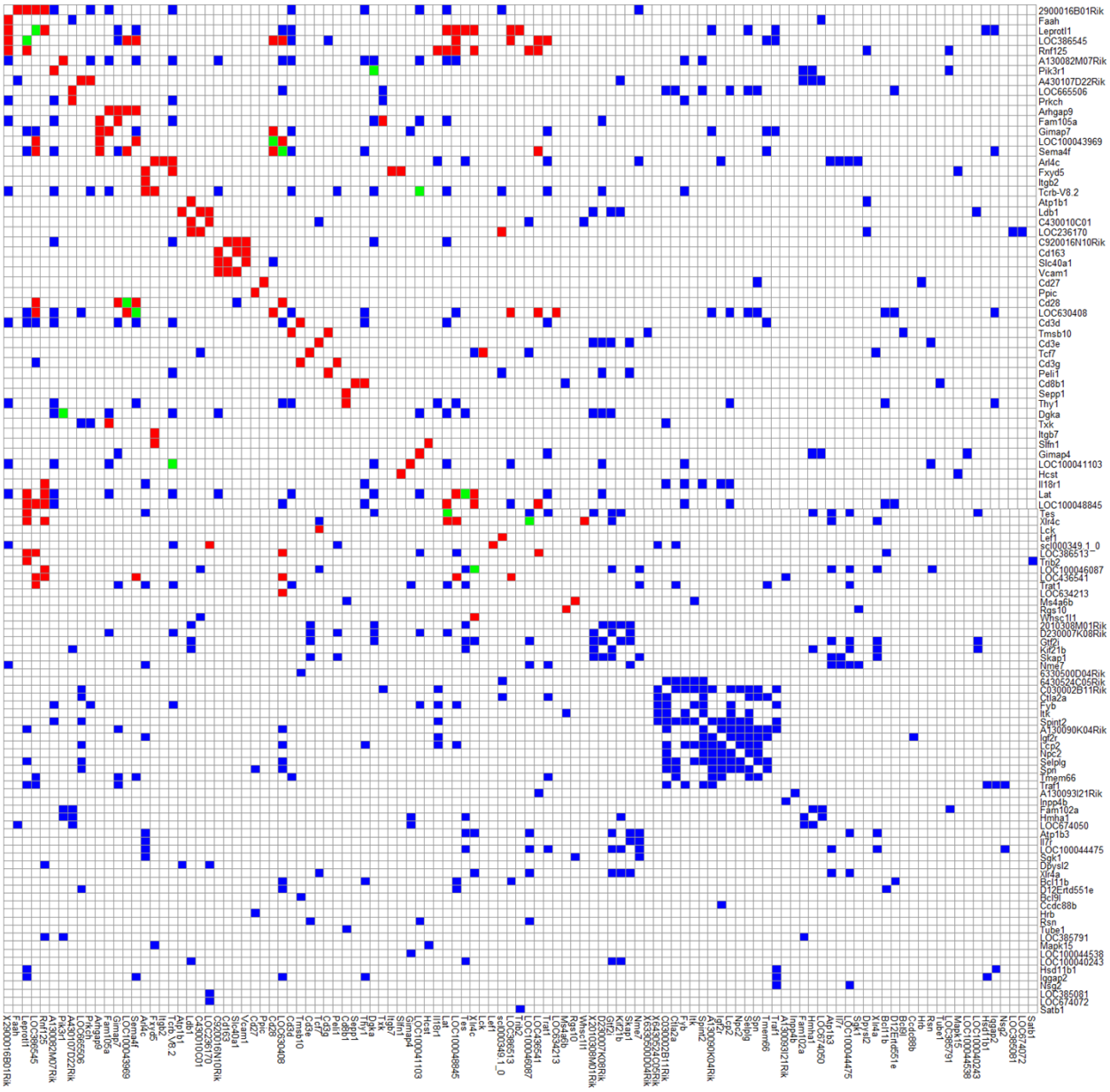

Fig 4. Adjacency matrices of gene co-expression for the two age related groups. The young adjacency matrix (red squares), the old adjacency matrix (blue squares) and elements that are conserved for both age-groups (green squares). Note that if you count the number of green squares above the diagonal, this is exactly seven which is how many conserved gene pairs are given in Table 3.

Consequentially, because only seven edges were conserved across the aging networks, most network edges were lost or gained with age. While the older mouse GCN saw an increase in total edges, 92% of the edges from the 2-month old GCN were not present in the 22/24-month old GCN, indicating 92% of the co-expression relationships established in young mice are absent in older mice. We identified 47 nodes present in the young network but whose co-expression relationships were lost with age in the senescent T-cells (Fig 5). Nodes in the older mouse GCN that gained new co-expression relationships not present in the younger mouse GCN can be viewed in Fig 6. Most of these genes with altered co-expression relationships encode for proteins involved in TCR/CD3 complex signaling and downstream signal transduction, such as the membrane receptor TCR alpha/beta chains, the CD3 complex (gamma, delta, epsilon CD3 chains), costimulation protein CD28, intracellular LCK, and Lat.

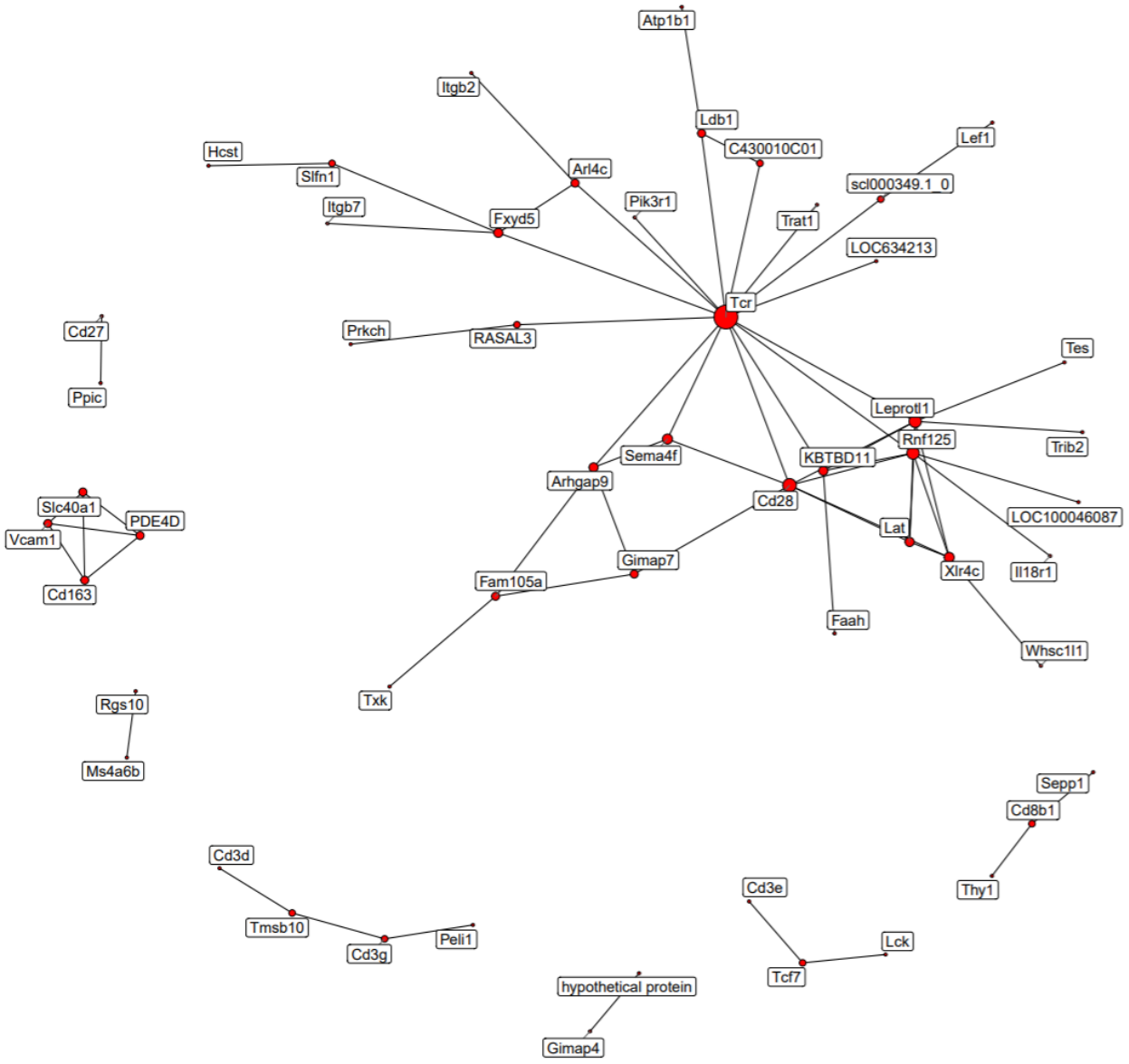

255

256 **Figure 5. Genes with co-expression relationships lost with age.** The young mouse GCN,

257 containing only edges that are not in the 22/24-month old mouse network. TCR probes were

258 merged into a single node to improve visibility.

259

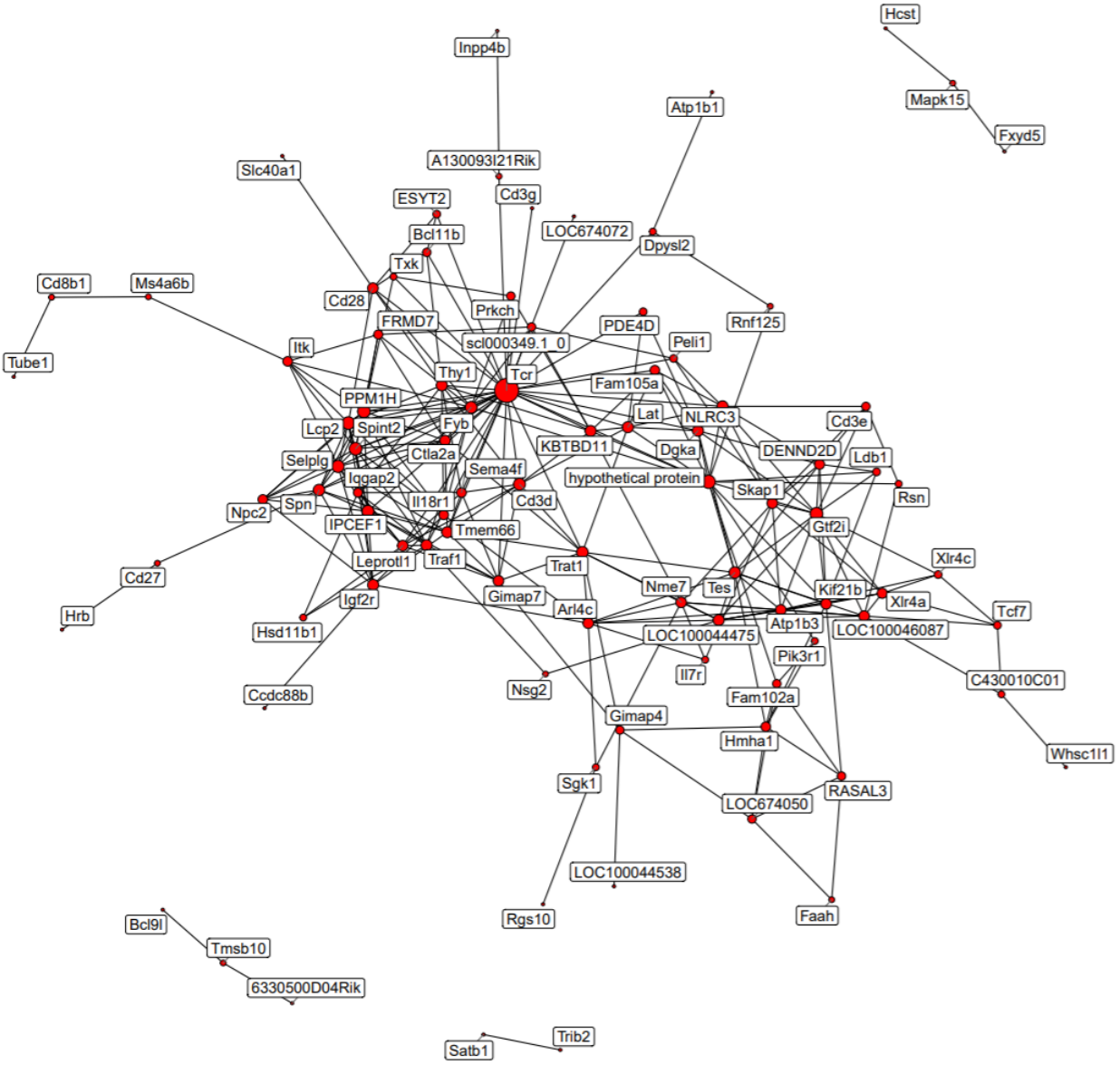

260

261 **Figure 6. Genes with co-expression relationships gained with age.** The older mouse GCN,

262 containing only edges that are not also present in the 2-month old mouse network. TCR probes

263 were merged into a single node to improve visibility.

264

265 **Network Centrality, Control and Node Power**

266 In order to better quantify the evolution of topology of the network of T-cell gene expression

267 during aging, we investigated the network centrality in the old and young mice network. The idea

of network centrality has a long history [50]. In general, network centrality speaks to the impact of a given node within a given network. A number of network centrality variables have been subsequently formulated and discussed in the literature. More recently, these methods were applied to the study of longevity-gene networks [35-38] as well as in a variety of other areas such as neurological mapping and social network analysis [51-57]. We begin with the concept of "degree centrality".

Degree centrality. *Degree centrality* counts how many neighbors a node has. A node has a neighbor if there is an edge directly connecting the node of interest to any other network nodes [35-38]. This definition argues that a network node is important if there are many nodes that are directly connected to it. From this definition, it follows that the given network node can affect the network to a greater extent, given that it has a high degree centrality. Degree centrality is the simplest of the centrality measures.

Table 4 illustrates the top ten gene-transcripts with the highest degree centrality in both networks. Of immediate note is the fact that the two young and old T-cell gene co-expression networks have totally different degree centrality nodes in the top 10 gene list, with the exception of TCR subunit gene LOC630408. Most genes with the highest centrality, including LOC630408, are identified as T-cell receptor components, which are highly diverse in the original spleen sample (S1 Table). In 2-month mice the degree centrality of TCR related genes is 6-10, while for the 22/24-month it doubles to 14 to 15, meaning that the TCR from senescent T-cells establish more links with other molecules. This suggests that the molecular relation is less specific (degeneracy), increasing the entropy of the system and decreasing the ordered organization established during development. Because degree centralities provide an overall view of the network connectivity, it

291 is reasonable to hypothesize the fact that the 22/24-month old network is three times larger than
292 the 2-month old network. We do note that network size differences may contribute to some of the
293 overall differences in degree centrality differences.

294 **Table 4: Top 10 highest degree centralities for the young and old mouse T-cell gene co-**
295 **expression networks.**

2 month Genes	Degree Centrality	22-24 month Genes	Degree Centrality
LOC386545	10	A130082M07Rik	15
Leprotl1	9	Lcp2	14
Rnf125	8	C030002B11Rik	14
LOC630408	7	Spint2	14
LOC100048845	6	Tcrb-V8.2	14
Sema4f	6	Gtf2i	14
LOC436541	6	LOC630408	14
Xlr4c	6	Selplg	13
Lat	5	A130090K04Rik	12
LOC100043969	5	Cd3d	12
		Fyb	12

Eigenvector centrality. *Eigenvector centrality* is another measure of the influence of a given node in a network. A high eigenvector centrality means that the given node is connected to many other nodes who themselves have high eigenvector centrality scores. You can think of this as follows: if a node is a big shot, then its high eigenvalue centrality provides a measure of how many other big shots is it connected to.

Table 5 lists the top 10 network nodes with respect to their eigenvalue centrality value. These genes represent the top 10 genes that are thought to exert general control over the whole network. It is straightforward to observe that the two GCNs showed clear differences in hub control dynamics as defined by eigenvector centrality values. We note that the values of the 2-month eigenvalue centralities are all greater than those in the 22/24-month network, meaning a more connected and organized network. Additionally, we note that the genes that control the 2-month network according to eigenvector centrality are entirely different from the older mouse network, save for TCR gene LOC630408, which also has a high degree centrality in both networks as reported in Table 4. Most of the transcripts with high eigenvector values in young mice are involved in the TCR and the CD28 co-receptor. Meanwhile, the highest ranked gene in the old mouse network is Lcp2, which encodes the adaptor protein SLP-76 that is a central figure in the TCR signaling pathway. Information regarding the other genes with high eigenvector centralities can be found in S1 Table.

318 **Table 5. Top 10 highest eigenvector centralities for the young and old mouse networks.**

2 month Genes	Degree Count	Eigenvector Centrality	22-24 month Genes	Degree Count	Eigenvector Centrality
LOC386545	10	0.40	Lcp2	14	0.27
Leprotl1	9	0.34	Spint2	14	0.26
LOC436541	6	0.30	Selplg	13	0.26
LOC100048845	6	0.30	C030002B11Rik	14	0.25
Rnf125	8	0.29	A130090K04Rik	12	0.24
LOC630408	7	0.28	LOC630408	14	0.23
Sema4f	6	0.26	Spn	11	0.21
LOC386513	4	0.23	A130082M07Rik	15	0.21
Xlr4c	6	0.22	Fyb	12	0.20
LOC100043969	5	0.21	Igf2r	10	0.18

Closeness centrality. *Closeness centrality* is a measure of the degree to which an individual node is near to all of the other nodes in a network. In Table 6 we provide the closeness centralities for the top 10 genes in both networks. First, we note that there are no common genes across the two networks. However, the functionalities of certain high ranking genes are conserved across the networks. For example, the first rank gene in the 2-month network is gene LOC386545 which is similar to T-cell receptor beta chain VNDNJC precursor (S1 Table). Meanwhile first rank gene in the 22/24-month old network is A130082M07Rik, a gene that functions as the T-cell receptor alpha chain variable 9D-3 region (S1 Table). This change in the top-ranked closeness centrality hubs suggests differences in T-cell clonal expansions in the two age-related groups, as has been previously described [24]. The functions of other high-ranking genes can be found in S1 Table.

Table 6. Top 10 highest closeness centralities for core the young and old mouse networks.

2 month Genes	Degree Count	Closeness Centrality	22-24 month Genes	Degree Count	Closeness Centrality
LOC386545	10	0.55	A130082M07Rik	15	0.38
Leprotl1	9	0.51	Trat1	11	0.38
LOC436541	6	0.48	Tcrb-V8.2	14	0.37
LOC100048845	6	0.47	Dgka	11	0.37
Sema4f	6	0.46	Lat	11	0.36
Rnf125	8	0.46	Tes	12	0.36
LOC630408	7	0.45	LOC100041103	10	0.35
2900016B01Rik	4	0.45	Cd3d	12	0.35

LOC386513	4	0.44	Fyb	12	0.35
Cd28	5	0.43	Arl4c	9	0.35

Betweenness centrality. *Betweenness centrality* represents the degree to which nodes stand in-between each other. One can say that betweenness centrality represents the control a specified node has over the network in that it finds nodes that act as bridges between nodes and – in a sense – these nodes may control the flow in the network. Such genes are often called bottleneck genes [58]. The higher the value of a node's betweenness centrality, the greater the degree of control the specified node exerts over the network.

Table 7 lists the top ten gene betweenness centrality values for both networks. Betweenness centrality values for the 22/24-month network are significantly greater that those of the 2-month network. In fact, they are 5-10 times those of the 2-month network. The gene Rnf12 is common across both networks; although it does not have the same betweenness rank. Rnf125 is believed to function as a positive regulator in the TCR signaling pathway. In the 2-month network, the highest ranked gene is once more the TCR gene LOC386545, while diacylglycoprotein kinase α (Dgka) has the highest ranking in the older mouse network. Other high-ranking gene information can be located in S1 Table.

Table 7. Top 10 highest betweenness centralities for the 2 and the 22-24 month old networks.

2 month Genes	Degree Count	Betweenness Centrality	22-24 month Genes	Degree Count	Betweenness Centrality

LOC386545	10	209.43	Dgka	11	1259.80
Leprotl1	9	135.15	Pik3r1	4	981.56
Rnf125	8	97.96	LOC385791	3	972
LOC436541	6	69.78	A130082M07Rik	15	889.60
Sema4f	6	67.67	Trat1	11	836.06
Arhgap9	4	66.15	Rnf125	2	820
LOC630408	7	56.64	Tes	12	762.45
Xlr4c	6	54.44	Arl4c	9	697.60
Cd28	5	53.85	Dpysl2	3	670
2900016B01Rik	4	51.29	Fyb	12	558.61

349

Network Stress and Eccentricity. The maximum distance between a node and all other nodes is called the *eccentricity* of that node; biologically, this can be said to represent the easiness for all other genes in a network to reach another particular gene. Consequently, the higher the eccentricity value, the easier it is for a given gene to be influenced by the rest of the network – or, conversely, the easier it is for that node to influence the rest of the network [59]. The higher eccentricity in old mice may influence the time of processes and increase the delay in intracellular interaction pathways affecting efficiency of the cells. Table 8 lists the genes with the highest eccentricity values in both networks. We note that the eccentricity values in the 22/24-month network were higher when compared to the 2-month network. Whsc1l1 is the only gene with a highly ranked eccentricity value shared by both the young mouse and old mouse networks (Table 8). Whsc1l1 is defined as nuclear receptor binding SET domain protein 3 that methylates Histone 3 (S1 Table). The gene with the highest eccentricity in the 2-month network is Whsc1l1, and the highest ranked gene in the 22/24-month network is LOC674072 which is similar to Ig heavy chain V region 441 precursor.

Table 8. Top 10 highest eccentricity values for the young and old mouse networks.

2 month Genes	Degree Count	Eccentricity	22-24 month Genes	Degree Count	Eccentricity
Whsc1l1	1	7	LOC674072	1	12
Txk	1	7	LOC385081	1	12
LOC100046087	2	6	Tube1	1	12
Trib2	1	6	Hrb	1	11

Xlr4c	6	6	Atp1b1	1	11
Tes	2	6	Cd8b1	2	11
Lat	5	6	LOC236170	3	11
Il18r1	1	6	Rgs10	1	10
Fam105a	3	6	Cd3g	1	10
Faah	1	6	Ccdc88b	1	10
			Whsc1l1	1	10
			Ms4a6b	2	10
			Cd27	2	10
			Hsd11b1	3	10
			Dpysl2	3	10

Stress of a node in a biological network is defined as the number of shortest paths passing through a given node. It can be used to indicate the prominence of a gene in holding together connecting regulatory genes in a network pathway. The higher the value, the more importance the node has in holding together communicating nodes [59]. We find that stress in the top ten highest stress nodes in the 22/24-month old group appears much higher than the highest stress nodes in the 2-month old group (Table 9).

Table 9. Top 10 highest stress values for the young and old mouse networks.

2-month Genes	Degree Count	Stress	Stress/ Weiner Index	22-24-month Genes	Degree Count	Stress	Stress/ Weiner Index
LOC386545	10	554	0.25	Dgka	11	6060	0.08
Leprotl1	9	316	0.14	Trat1	11	5906	0.08
Rnf125	8	252	0.11	Tes	12	5496	0.07
Sema4f	6	214	0.10	A130082M07Rik	15	4750	0.06
Arhgap9	4	212	0.10	Arl4c	9	4066	0.05
LOC436541	6	208	0.09	Itk	7	3936	0.05
LOC100048845	6	186	0.08	Pik3r1	4	3886	0.05
Cd28	5	158	0.07	LOC385791	3	3804	0.05
Xlr4c	6	158	0.07	Fyb	12	3586	0.05
Fam105a	3	142	0.06	Rnf125	2	3180	0.04

373

374 **Weiner index.** The *Weiner index* provides valuable context for these stress measures (Table 2).
375 The Weiner index is the sum of the number of shortest paths in a network. We can use the
376 Weiner index as a normalization factor. Comparing the ratio of the highest stress nodes to the
377 Weiner index, we can see that the highest stress nodes in the older mouse group actually have a
378 lower proportion of shortest paths in the total network as compared to the 2-month old group
379 (Table 9). As a result, the genes with high stress values in the 2-month old group can be seen to
380 have a greater impact on network connection than genes of high stress in the 22/24-month old
381 group. Rnf125 is the only gene with high ranking in both networks and, as noted above, it is the
382 only gene with high betweenness centralities shared by both networks as well. Rnf125 is similar
383 to T-cell RNG activation protein 1. The function of genes with high-ranking stress values can be
384 found in S1 Table.
385

Network Influence Measures. There are three *influence measures* of importance, where influence can be thought of as a measure of which nodes have power in a given network. These influence measures are given by: *(1) Local influence, (2) Indirect influence and (3) Total influence* [60]. The local influence of a node can be thought of as how much the given node affects its one-hop neighbors; the nodes directly connected to a given node by an edge. The indirect influence may be thought of as how much the given node affects its two-hop neighbors, nodes whose paths are connected by a single node mediating node. Lastly, the total measure of influence is defined as the weighted sum of the local and indirect influences. The ten highest local, indirect, and total influence values for the young and old mouse networks can be found in Tables 10-12. Again, a gene encoding TCR (LOC630408) is the only transcript in the top highest local, indirect, and total influence values across both networks. The identity of genes in the highest rank ordered influence values exclusive to each network can be found in S1 Table.

Table 10. Top 10 highest local influence values for the young and old mouse networks.

2 month Genes	Local Influence	22-24 month Genes	Local Influence
LOC386545	0.99	A130082M07Rik	1.16
Leprotl1	0.94	Lcp2	1.15
nf125	0.89	LOC630408	1.15
LOC630408	0.86	Gtf2i	1.15
LOC100048845	0.83	C030002B11Rik	1.14
Sema4f	0.82	Spint2	1.14
LOC436541	0.82	Tcrb-V8.2	1.13
Xlr4c	0.80	Selplg	1.12
LOC100043969	0.76	Cd3d	1.09

Lat	0.762	A130090K04Rik	1.09

Table 11. Top 10 highest indirect influence values for the young and old mouse networks.

2 month Genes	Indirect Influence	22-24 month Genes	Indirect Influence
Leprotl1	0.83	LOC630408	1.23
LOC386545	0.82	A130082M07Rik	1.23
LOC100048845	0.76	Spint2	1.20
LOC630408	0.75	Lcp2	1.20
Rnf125	0.73	Selplg	1.18
LOC436541	0.73	A130090K04Rik	1.17
Xlr4c	0.72	Tcrb-V8.2	1.16
Sema4f	0.72	Cd3d	1.16
LOC100043969	0.68	Gtf2i	1.14
Lat	0.673789	C030002B11Rik	1.14

Table 12. Top 10 highest total influence values for the young and old mouse networks.

2 month Genes	Total Influence	22-24 month Genes	Total Influence
LOC386545	0.92	A130082M07Rik	1.19
Leprotl1	0.89	LOC630408	1.18
Rnf125	0.82	Lcp2	1.17
LOC630408	0.82	Spint2	1.16
LOC100048845	0.80	Gtf2i	1.14
LOC436541	0.78	Selplg	1.14
Sema4f	0.78	Tcrb-V8.2	1.14

Xlr4c	0.77	C030002B11Rik	1.14
LOC100043969	0.73	A130090K04Rik	1.13
Lat	0.73	Cd3d	1.12

Clustering Coefficient Analysis. The *clustering coefficient* of a node is a measure of the degree to which genes in a network tend to cluster together around the particular gene [28]. The mean clustering coefficient for each network, defined as the sum total of all clustering coefficients divided by the number of nodes, is found in Table 13. The mean clustering coefficient for the 2-month network is 0.251, while the mean for the 22/24-month is 0.335. The genes with the highest clustering coefficients in the 2-month and 24-month core networks can be found in Table 13. None of the genes with the highest clustering coefficients in the 2-month network were in the highest ranked genes for the 22/24-month network.

Table 13. Top 10 highest clustering coefficients for core the young and old mouse networks.

2 month Genes	Degree Count	Clustering Coefficient	22-24 month Genes	Degree Count	Clustering Coefficient
Tes	2	1.0	C920016N10Rik	4	1.0
LOC100046087	2	1.0	Hsd11b1	3	1.0
LOC100043969	5	0.7	Faah	2	1.0
Lat	5	0.7	Npc2	7	0.90
LOC386513	4	0.67	Fam105a	7	0.86

LOC100048845	6	0.6	LOC100040243	4	0.83
Sema4f	6	0.6	Ldb1	4	0.83
Cd28	5	0.6	Xlr4c	5	0.8
LOC630408	7	0.48	Il7r	3	0.67
LOC436541	6	0.47	D12Ertd551e	4	0.67
			Tcf7	4	0.67

Fig 7 illustrates the spread of clustering coefficients *vs*. degree (k). Blue points indicate older mice, while red points indicate the younger mice. Of immediate note is that the 22/24-month network has a wider range of clustering coefficients compared to the 2-month network. Meanwhile, the 2-month network clustering coefficients are more compactly distributed. This apparent increase in highly interconnected genes in the old mouse GCN is consistent with the observed large core network that makes up the old mouse GCN (Fig 3).

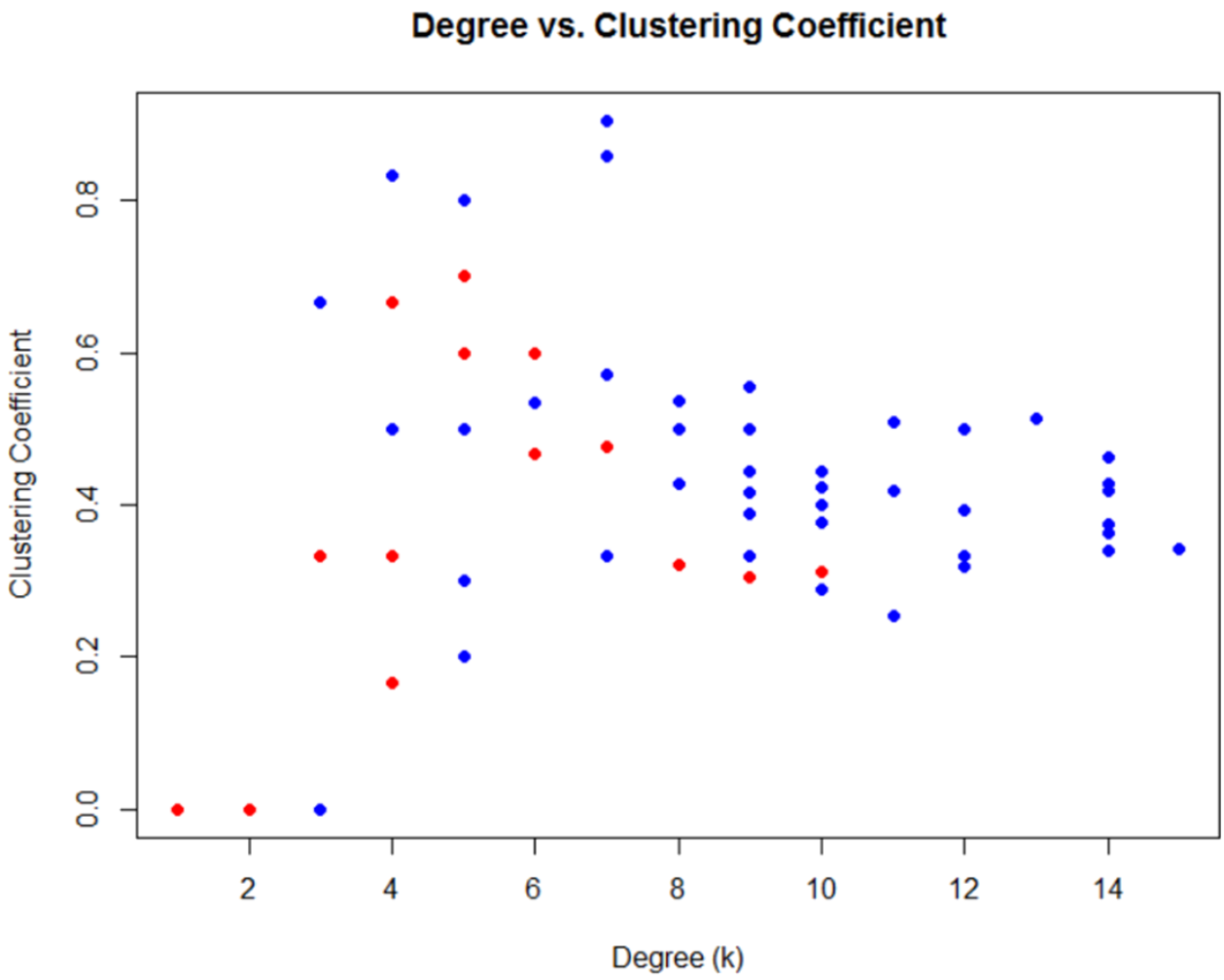

Fig 7. Plot of clustering coefficient versus network degree for the network gene co-expression in the two, mouse age-groups. Red points correspond with the 2-month age group, while blue corresponds with the 22/24-month age-group. It is straightforward to observe the large scattering of co-expression gene pairs in the 22/24-month age-group, while this is not the case for the 2-month old age group.

The program MCODE was used to find tightly connected subnetworks within a core network (http://apps.cytoscape.org/apps/mcode). MCODE is used to find clusters in network data

based upon core clustering coefficients. It can determine pathways of biological significance in protein and gene networks. MCODE found four tightly linked subnetwork clusters in the 2-month old network, and six tightly linked clusters in the 22/24-month old network (S3 Fig). The identity of genes involved in these subnetworks can be found in S1 Table.

Centrality Analysis of Conserved Gene Pairs. Finally, we summarize the rankings of the conserved co-expressed gene pairs (see Table 3) in Table 14. We note that Leprotl1 and the TCR gene LOC386545 have most of the highest rankings among the genes that are conserved between the young and the old networks.

Table 14. Centrality rankings of genes with conserved co-expression in both networks.

	Degree		Eigenvector		Betweenness		Closeness		Clustering		Eccentricity		Stress		Local Influence		Indirect Influence		Total Influence	
Gene Names	Y	O	Y	O	Y	O	Y	O	Y	O	Y	O	Y	O	Y	O	Y	O	Y	O
Sema4f	6	-	7	6	5	-	5	-	7	-	-	-	4	-	6	-	8	-	8	-
LOC630408	4	7	6	-	7	-	7	-	9	-	-	-	-	-	4	3	4	1	4	1
LOC386545	1	-	1	-	1	-	1	-	-	-	-	-	1	-	1	-	2	-	2	-
Leprotl1	2	-	2	-	2	1	2	-	-	-	-	-	2	-	2	-	1	-	1	-
PiK3r1	-	-	-	-	-		-	-	-	-	-	-	-	7	-	-	-	-		-
Dgka	-	-	-	-	-	1	-	4	-	-	-	-	-	1	-	-	-	-	-	-
Loc1000043969	10	-	10	-	-	-	-	-	3	1	-	-	-	-	9	-	9	-	9	-
CD28	-	-	--	-	9	-	8	-	8	-	-	-	8	-	-	-	-	-	-	-
Tcrb-V8.2	-	5	-	-	-	-	-	3	-	-	-	-	-	-	-	7	-	7	-	7
LOC100041103	-	-	-	-	-	-	-	-	-	-	-	-	-	-	-	-	-	-	-	-
Tes	-	10	-	-	-	7	-	6	1	-	6	-	-	3	-	-	-	-	-	-
Lat	9	-	-	-	-	7	-	5	4	-	7	-	-	-	10	-	10	-	10	-
Xlr4c	8	-	8	-	8	-	-	-	-	8	5	-	9	-	8	-	7	-	7	-
LOC100046087	-	-	-	-	-	-	-	-	2	-	3	-	-	-	-	-	-	-	-	-

Column headers indicate the age of the mice from which the samples were taken (Y: 2-month, O: 22/24 month). A dash indicates that the given gene was not in the top 10 genes for that centrality variable. The braces correspond to the nodes (genes) at the end of the edges in Table 3. We note that the edge with the gene pair LOC386545 (similar to T-cell receptor beta chain VNDNJC precursor) – Leprotl1 (Leptin receptor overlapping transcript like 1) appears across all centrality measures, except for clustering and eccentricity, in that it always ranks 1-2 for the young mouse

cells but not for the old mouse cells. This makes this edge and nodes pair a very powerful component in the young network.

Scale Free Analysis

Scale-free analysis has significance in biological networks [61-63]. Scale-free networks are networks whose degree distribution follows a power law with a power parameter that typically falls in the interval 2-3, however, it may fall outside this interval [64]. Analysis of our two network architectures showed that the two-month old GCN is of scale free type, while the scale-free network structure was weaker for the older mouse GCN. Power curve analysis, fitting the function $P(k) = Ak^{\gamma}$ to the P(k) for each network, showed that the younger mouse GCN followed a strong power law behavior (R^2 = 0.9192, p-value < 0.001, Fig XA), while the older mouse group demonstrated a weaker power law behavior (R^2 = 0.4944, p-value <0.01, Fig XB).

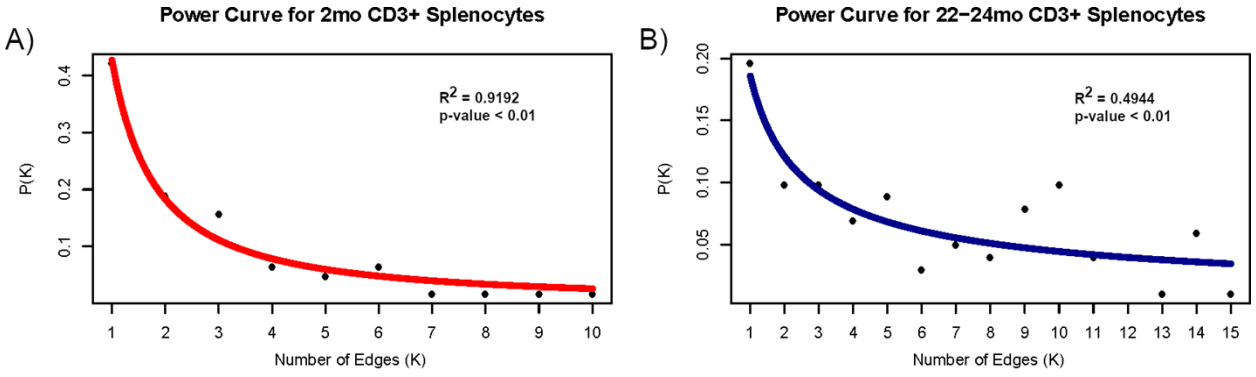

Fig 8. Power curve analysis of the two age-related networks based on degree distribution. Fitting the curve $P(k) = Ak^{-\gamma}$: Probability of degree frequency ``k'' in (A) the two-month-old mice group can be moderately predicted by power law analysis (R^2 =0.9192, p-value = 1.2×10^{-5},

log P(k) = -1.58log(k) - 0.25). The predictive strength of this model was weakened in (B) the 22/24-month old group (R^2= 0.4944, p-value=0.003452, log P(k) = -0.7461log(k) - 0.6883).

Discussion

The gene co-expression network analysis of a 130 gene signature from young and old mice yielded a variety of interesting insights and conclusions about aging. First, we observe an alteration of the TCR signaling pathway in old mice, where the TCR complex and CD28 co-stimulatory molecules upstream the pathways are particularly affected. The RNA encoding the proteins present on the membrane of T-cells required for full T cell activation were co-expressed in the young mouse GCN, while this was not true of the old mouse network. The small core network of TCR-related genes in the young mice reveals that gene co-expression for proteins involved in TCR signaling are stable across the three strains of mice, suggesting the core network is robust across the genetic variation in mice strains.

Further, while the network of young mice is well organized and reflects controlled development across each genetic background, those of old mice appears more stochastic. We found a 255% increase in the number of edges in the 22/24-month old network when compared to the 2-month old network. However, we only found seven edges in the 22/24-month network that were also found in the 2-month network. This suggests that many of the edges in the 22/24-month old GCN were the result of novel co-expression relationships likely gained as a result of age.

Power law analysis suggests a deterioration in network organization in the old mouse network compared to the young mice. Analysis by power law demonstrated the 2-month old network was a scale-free network type, while the 22/24-month old network was not. Scale-free

504 networks are frequently more robust to perturbations than are other network architectures,
505 indicative of both complexity and organization. The scale-free network structure of the 2-month
506 GCN is typical of most biological networks [62]. Scale-free network types may provide an
507 advantage to biological systems that are subject to damage by mutation and/or viral infection. The
508 scale-free network structure of the young CD3+ T-cells indicates that transcription of genes is
509 tightly regulated in the splenocytes of 2-month old mice that are fully immunocompetent. Decrease
510 in scale-free structure in the co-expression patterns of the 22/24-month old mouse splenocytes
511 suggests that this control is decreased with age.

512 This change in network architecture has interesting implications for the regulatory behavior
513 of genes in older T-cells. Because the major signal transduction from the TCR complex and CD28
514 is disturbed, the expression of the internal cell molecules is consequently perturbed in senescent
515 T-cells. That the 22/24-month old mouse splenocytes see an increase in correlation at the expense
516 of more organized network structures suggests T-cell regulation and immune behavior is
517 diminished. Indeed, in the same series of FVB and B6 mice, we previously quantified by flow
518 cytometry and mathematical models that the T-cell cycle transition rates and proliferation/death
519 rates were altered in 18 month-old mice as compared to 2 month-old mice [24]. And while we
520 have no direct evidence for the implication of these results with respect to human immune T-cell
521 dynamics, we do know that human T-cell populations are also altered with age, and that there are
522 a variety of other changes in T-cell behaviors in humans: in particular, changes in signal
523 transduction in T-cells, and the promotion of long lived T-cells with less efficient function and
524 inflamm-aging [65], even while the total lymphocyte maintenance is preserved [66].

525 Changes in network structure with age also reveal differential co-expression relationships
526 in several key gene pathways. For example, expression of Transcription Factor 7 (TCF7) is

important for T-lymphocyte differentiation. This transcription factor is essential for the proliferation of early DN thymocytes, the survival of DP cells, positive/negative selection, as well as for the creation of the CD3/TCR complex and the cell cycle control, and, in peripheral tissues, for the orientation to the TH2 pro-inflammatory pathways and activation of memory CD8 T-cells [67]. We previously quantified increased time spent in gap phases of the cell cycle leading to decreased division rates in immature DN and mature CD3hi DP thymocytes in FVB mice: the time spent in gap phases in G0/G1 and G2/M2 from DN to CD3hi DP increases from 10.2 days in young B6 mice to 28 days in young FVB mice, and even up to 58 days in 18 months old FVB mice. These proliferation rates were decreased in thymus and the spleen in FVB mice, as compared to B6 mice, contributing to acceleration of the thymic involution [24]. We also found increased occurrence of oligoclonal expansions of CD8 T-cells in FVB old mice [25].

Additionally, we previously observed an increase in differentiation of Tregs in old FVB mice but defective proliferation in the spleen. Interestingly, such a defect could be related to a deficiency of TCF7 in old FVB mice. Such a defect would lower the threshold to differentiate Tregs.

In the 2-month old network, TCF7 falls in a three-node island with genes Lck and CD28e. Transcription of TCF7 is previously reported to correlate with the expression of both Lck and CD28e [68-69], and the 2-month old network indicates these biological relationships. This co-expression linkage is lost in the 22/24-month old GCN, where the TCF7 node loses connections to Lck and CD28e and gains co-expression relationships with genes Xlr4a, Xlr4c, C430010C01 and TCR probe LOC10004608. This suggests massive alteration in this gene regulatory pathway with age. Because TCF7 increases Th2 differentiation and inflammation, these changes in co-

549 expression relationships might contribute to inflammation [67], in addition to changes in T-cell
550 populations observed with age [24] [25].

551 However, it is not fully known if the increase in co-expression relationships across the old
552 mouse GCN serves any biological function, or whether these changes have a detrimental or
553 compensatory impact on gene expression behavior in old T-cells. Some results in the original
554 signature, however, suggested biological relevance with what is currently known about T-cells
555 during immunosenescence. The old mice had lower expression of these genes related to TCR
556 activation, such as CD3, VB8.2, co-stimulation molecule CD28, early activation molecule CD69,
557 adhesion molecule VCAM1, Thy1, receptor to lymphokines IL-7R, and CD27. The TCR/CD3
558 complex receptor-to-antigen interaction, and the downstream signal transduction involving
559 LCP2/SLP-76 recruitment, binding GADs and lat, the co-stimulatory signal via CD28 and its
560 cytoplasmic tail binding, and CTLA-4 are all affected by age [49-50]. We observed that the aging
561 signature affects several functions related to hematopoietical system as seen in IPA (S2 Fig),
562 related not only to activation (TCR/CD3/CD69), but also binding and adhesion/interaction
563 (VCAM1). Pathway enrichments for the genes appearing in both networks also suggest these genes
564 play a role in changes in the immune system with age (Fig 2).

565 Differences in network hubs within the two age-related networks can be used to infer more
566 about changes in key gene pathways that may be attributable to age. Hubs are important
567 determinants of system functions in a biological network; in co-expression networks, deletion of
568 a hub gene is likely to result in cell death [70]. Across the two age-related GCNs, very few of the
569 hub genes as defined by degree, eigenvector, betweenness, and closeness centralities, as well as
570 the influence measures, clustering coefficient, eccentricity, and stress values, were the same
571 (Tables 4-13). Further, very few hub genes in the older mouse network were highly rated across

572 the different node centrality measures, while there was more consistency and less variety of highly-
573 rated genes in the young mouse network. This suggests the hubs in the young mouse network have
574 overall more control, importance, and power over the network structure compared to the old moue
575 network hubs.

576 Two genes with a co-expression relationship conserved across both networks, Sema4f
577 (sema domain, immunoglobulin domain (Ig), TM domain, and short cytoplasmic domain) and
578 TCR (gene LOC630408, T-cell receptor alpha chain V region CTL-L17 precursor), appeared in a
579 high rank across multiple hub measures for both age-related networks, as summarized in Table 14.
580 Additionally, both Sema4f and TCR/LOC630408 were incorporated into a tightly clustered
581 MCODE subnetwork for the young mouse group (S3A Fig), but not the old mouse network (S3B
582 Fig). That the co-expression relationship between these genes is conserved in both networks
583 implies this expression relationship has important biological function, or a precursor to these genes
584 serves as an important biological mediator. Further, that these genes serve as important hubs in
585 both networks suggests a biological importance of both genes in both young and old splenocytes,
586 although the lower centrality rankings and lack of MCODE clustering for the older mice suggests
587 these genes have a diminishing role with age.

588 We note that the edge of co-expression with the gene pair TCR (LOC386545 similar to T-
589 cell receptor beta chain VNDNJC precursor) – Leprotl1 (Leptin receptor overlapping transcript
590 like 1) appears across all centrality measures, except for clustering and eccentricity, in that it
591 always ranks 1-2 for the young mouse cells but not for the old mouse cells (Table 14). This makes
592 this edge and nodes pair a very powerful component in the young network. The Leprotl1 gene
593 encodes a homologue of the leptin membrane receptor. Leptin is an adipokine than regulates
594 appetite and food intake but also is involved in T-cell differentiation and regulation of adiposis

595 and the immune system. Notably, the exponential rise in metabolic and autoimmune diseases with
596 age might be related to metabolism and leptin. Leptin is secreted by both adipocytes and T-cells,
597 in particular this autocrine production by Treg cells can down-regulate T-cell proliferation during
598 immune response and prevent inflammation [71]. Interestingly, leptin inhibits the proliferation of
599 Treg cells [72] and their control of inflamm-aging. The leptin receptor is further involved in
600 JACK2 STAT-3 orientation and Thelper cell activation, promoting Th17 differentiation but
601 inhibiting Treg differentiation. Moreover, leptin promotes the proliferation of naïve T-cells but
602 inhibits the proliferation of memory T-cells. The Leprotl1 gene is highly expressed in FVB mice,
603 as is CD69, an early activation marker of T-cells. Notably, by contrast, these proteins are lesser
604 expressed in B6 and BALB/c mice. The conservation of co-expression of Leprotl1 and the TCR
605 gene across the age-related networks stresses the biological importance of this co-expression
606 relationship, but changes in network hub rankings suggests the downstream pathways of the leptin
607 receptor are altered with age.

608 In conclusion, we found significant deterioration of network organization when comparing
609 the 2-month network to the 22/24-month network and observed changes in hub genes suggesting
610 changes in TCR signaling and co-stimulation through CD28 in the two age-related groups. This
611 analysis provides evidence of a defective organization of transcription in older peripheral T-cells.
612 This dis-organization is suspected to increase delays in T-cell regulation pathways and inhibit the
613 biological activity of CD3+ lymphocytes, while other cells die and cannot be quantified here. In
614 addition, the identification of hub genes for network expression in the young and old mouse groups
615 help identify genes important to healthy cell function and deteriorating function with age,
616 providing opportunities to approach these genes as potential therapeutic targets to help aging

617 patients. Human orthologs of the genes used in this analysis (S1 Table) could help to understand
618 human aging in lymphocytes.

619 **Limitations**

620 Previous GCN research using AGEMAP data found a decrease in gene co-expression with
621 age in mice across multiple tissue types [38]. This contrasts with the results of this study, which
622 found a nearly 255% increase in the number of edges in the old mouse group GCN as compared
623 to the younger mouse group. There are several factors that may contribute to this result. One
624 component may be experiment design: the AGEMAP study utilized tissue from only C57BL/6
625 mice, both male and female, instead of using exclusively female mice from three separate mouse
626 lines. Additionally, samples in the AGEMAP study were extracted from mice at ages 16 and 24
627 months, as opposed to 2 and 22-24 months. The size of both datasets may also contribute in
628 different, limited results (10 mice per age/sex, as opposed to 11-12 mice per age group). Finally,
629 an important factor is that the AGEMAP study did not look at co-expression in peripheral T-cells,
630 which may behave differently from other cell types across the aging process. Indeed, T-cells are
631 permanently selected to survive and to divide through the TCR complex and co-stimulation
632 pathways, or they undergo apoptosis if too many default signals occur (as during the cell cycle).
633 Results by Vibert & Thomas-Vaslin [24] show that across ages and genetic backgrounds, immature
634 T-cells in the thymus and mature T-cells in spleen show a decrease in T-cell proliferation with
635 early T-cell differentiation, compensated by an increase of proliferation of effector/memory T-
636 cells in spleen, that often correlates with oligoclonal T-cell expansions [25]. Because 92% of the
637 edges in the younger mouse GCN are lost in the older mouse GCN, differences in network
638 architecture may be attributed to age-related changes in key biological pathways in CD3+
639 splenocytes.

Another limitation of this study is that the dataset contains expression data from an array of T-cell subtypes not separated based on differentiation markers. Therefore, changes in co-expression behavior attributable to naïve, CD4+, or CD8+ cells cannot be discerned through this analysis.

In humans CD4, CD8, and CD3 T-cells present some overlap in gene expression during an immune response [73]. While thymic output of T-cells decreases with age, it is known that in some cases, older mice still produce naïve T-cells [25, 74]. This suggests the spleen dataset for the older mouse network may include expression data from both new and senescent T-cells, cell types which might demonstrate differential gene co-expression and proliferation propensity [30]. However, the production of naïve T-cells in mice is diminished around 5-10 fold in 18 old months mice, as it is also the case in human at midlife, at about 50 years [25]. In humans, there is 95% gene similarity between naïve and memory T-cells [75]. In C57BL/6 mice, both isolated naïve and memory CD4 T-cells from old mice present different alteration in gene expression, but both expression profiles are turned to inflammation [76]. Additionally, naïve and memory CD4 T-cells share fewer genes in common in old than in young mice, suggesting also a deterioration of these transcriptional pathways with aging. Over time, naïve T-cells may also increase their ability to persist [77]. Certain transcriptional changes, such as an increase in metabolism during the transition from naïve to effector T-cells, could not be accessed here [78].

The other limitation is the evolution of Treg cells, which represent only 1% of lymphocytes (about 5-10% of CD4), but their numbers increase with aging while their functionalities and regulatory functions decrease with the secretion of IL-2. In young mice, IL-2 at low doses stimulates Treg and negatively regulate T-cell proliferation, while at high doses Il-2 upregulates

the proliferation of T-cells [25]. The role of Tregs in adipose-associated tissues is also correlated with increasing expression of anti-inflammatory genes such as IL-10.

Of course, these different age-related alterations in cell behavior are not specific to T-cell subtypes. Studies have found biomarkers of aging and senescence in other tissues in mice that suggest there may be cell-specific changes in gene expression with age [79]. Due to these variations, further investigations into co-expression in T-cells based on cellular age and T-cell subtype are necessary.

Interestingly, results by Vibert & Thomas-Vaslin show T-cell proliferation/death rates has higher inter-individual variation in the older mouse group when compared to the younger mouse group [24]. This may have an impact on the increased co-expression relationships evident in the old mouse GCN. Genes that are co-expressed in the old mouse group may also vary, resulting in the increased representation of nodes and edges in the old mouse GCN. This suggests co-expression pathways affected by age in CD3+ splenocytes vary based on genetic background and individual influences, demonstrating the need for future investigation into co-expression relationships in T-cells with age.

Methods

Mice

C57BL/6J (B6), BALB/cByJ and FVB/N (FVB) mice were obtained from Charles River Laboratories at 4 weeks of age, maintained in SPF conditions in our animal house (Centre d'Exploration Fonctionnelle Pitié Salpétrière–Paris) and fed with the same diet. Mice were sacrificed at 2 and 22-24 months of age. Mice were manipulated according to European council directive 86/609/EEC of 24 November 1986 and with the approval of an ethics committee.

684 **Sorting of CD3+ cells for mRNA preservation**

685 Mice were sacrificed by cervical dislocation and spleens were collected. Cell suspensions
686 were obtained by mechanical disruption of organs in PBS + 3% newborn calf serum at 4°C, were
687 then washed, and viable cells were counted by trypan blue exclusion. CD3+ cells were isolated by
688 positive selection using anti-CD3 biotine followed by streptavidin beads labelling and passage
689 through LS magnetic Miltenyi column to recover fixed cells.

690 **Transcriptomics profiling**

691 Gene expression was measured in CD3+ splenocytes extracted from FVB/N (n=4 young
692 and n=3 old), C57BL/6N (n=4 young and n=3 old), and BALB/cByJ (n=4 young and n=5 old)
693 mice. The young mice were age two months old. The old mice were age 22-24 months old.

694 One million purified cells were lysed in Trizol (Invitrogen) and immediately transferred to
695 -80°C for storage. Samples were then lysed and total RNA was purified using Trizol (Invitrogen)
696 according to the manufacturer's instructions. RNA yield was assessed using a NanoDrop 1000
697 spectrophotometer (NanoDrop Products, Thermo Fisher Scientific). RNA integrity was assessed
698 using an Agilent Bioanalyzer showing a quality RNA integrity number of 8–10 (Agilent
699 Technologies). The RNA was processed using the Illumina TotalPrep RNA Amplification Kit
700 Protocol according to the manufacturer's protocol. Briefly, labeled complementary RNAs (cRNAs)
701 were hybridized overnight with Illumina MouseWG-6 v2.0 Expression BeadChip arrays. The
702 arrays were then washed, blocked, stained and scanned on an Illumina BeadStation following the
703 manufacturer's protocols. Illumina BeadStudio software (Illumina) was used to generate signal
704 intensity values from the scans as previously described [85].

705 **Filtration and normalization of transcriptomics data**

706 Microarray probes were filtered out from the analysis if their expression was below the
707 detection limit (p-value < 0.05) in at least 2 out of 3 samples in both the microenvironment and
708 control groups. Next, data were log-transformed and normalized by the quantiles method using the
709 R package limma v3.28.4.

710 **Identification of specific molecular signatures**

711 Specific molecular signatures were generated and statistically tested using the ICA/GSEA
712 method [86], a strategy that combines the Independent Component Analysis (ICA) and the Gene
713 Set Enrichment Analysis (GSEA). ICA, an unsupervised method, separates gene expression into
714 non-Gaussian and statistically independent components. From each component, two potential
715 molecular signatures were defined as those genes having extreme loading on components.
716 Signatures were assembled in a database and tested for their enrichment in GSEA using the "pre-
717 ranked list" option. Gene lists were sorted according to the value of the limma's eBayes statistic.
718 We used the weighted scoring scheme to compute the enrichment score. GSEA provides a
719 normalized enrichment score, permutation p-value and FDR q-value indicating the significant
720 level of each signature. A detailed explanation of GSEA can be found in Subramanian et al. [87].
721 Based upon altered gene expression in all aging mice, a total of 130 immune-related genes from
722 the signature with the highest p-value (a signature named C2-5) was chosen for analysis among
723 900 signatures [24]. This signature was chosen since it allows to distinguish young from old mice,
724 independently of their genetic origin. The resulting gene expression data was then grouped by age
725 (12 young mice and 11 old mice) and gene co-expression.

726 **Gene co-expression networks construction**

727 The Spearman rank correlations (r_s) measuring co-expression levels were standardized by
728 squaring r_s, and the coefficient of determination R^2 was used for network construction. This
729 transformation ensures that the co-expression dataset included both strong positive and strong
730 negative expression correlations. Significant co-expressed genes incorporated into network
731 construction were defined as correlated gene pairs which had an $R^2 > 0.8$ and a p-value < 0.01
732 [84]. The Python scripts used to filter this dataset based on these parameters are available on
733 GitHub (http://github.com/mairml/network-analysis).

734 **Gene functional enrichment analysis**

735 Human orthologues for the *mus musculus* genes, in the two networks, were determined
736 using OrthoDB (http://orthodb.org). Additional functional annotations were retrieved from
737 GenBank. All orthologues and functional annotations are provided in **S1 Table**.

738 MSigDB from GSEA was used to determine genes in each network that share common
739 biological pathways in KEGG and REACTOME databases
740 (http://software.broadinstitute.org/gsea/msigdb/annotate.jsp). Gene overlaps were calculated
741 using an FDR of less than 0.05 in the Novartis human tissue compendium. Ingenuity Pathway
742 Analysis was additionally utilized to analyze pathway enrichments in the dataset.

743 **Network topological analysis**

744 Both the young and old mice networks were visualized using Cytoscape version 3.6.0
745 (http://cytoscape.org/download.php). The following network properties were calculated: network
746 diameter, eigenvalue and betweenness centrality, clustering and closeness, network stress, network
747 radius, network eccentricity, clustering, local influence, indirect and total influence. Built-in

Cytoscape network analysis tools were used to find the mean shortest path, mean edge count, network diameter, radius and clustering coefficients for both GCNs. CentiScaPe version 2.2 was used to calculate centrality measures for each of the two networks (http://apps.cytoscape.org/apps/centiscape). The Grafman software was used to cross-check analysis results. The Grafman software is available from Bonchev [85]. Cytoscape plugin MCODE (http://apps.cytoscape.org/apps/mcode) was used to identify network clusters. Node influence was calculated using the algorithms discussed by Qiao *et al*. [60]. Adjacency matrices were calculated in Python (available at GitHub) and visualized in using the R package pheatmaps (http://cran.r-project.org/package=pheatmap). Distance matrices were calculated in Python (available at GitHub). Frequency distribution for each network was calculated using a Python script (available at GitHub). The frequency distributions were then scaled to probabilities and subsequently plotted in R v 3.1.1. Log-log plots associated with each of the model forms were used to estimate the model parameters. All parameters were estimated using linear regression on the log-transformed data [35-36].

Acknowledgments

We would like to thank Dr. Phuong Pham (Sorbonne Université- INSERM UMRS 959 Immunology, Immunopathology, Immunotherapy CERVI, Pitié-Salpêtrière Hospital, Paris, France) for providing the C2-5 signature, for the conversion of microarray data into correlation matrices and for the constant support, and advice throughout the execution of this project. We would also like to thank Dr. Danail Bonchev (Virginia Commonwealth University) for his generous assistance in providing us with Grafman software as well as for his time in discussing network mathematics with us. Moreover, we wish to thank him for his assistance with some of the network calculations. Lastly, we would like to thank Dr. Wei Shan (Beihang University, China)

771 and his team for his sharing their software for the calculation of local and global node power in a
772 network.

773

774 References

775 1. Lavelle C, Berry H, Beslon G, et al. From molecules to organisms: towards multiscale
776 integrated models of biological systems. Theoretical Biology Insights. 2008;1:13–22.
777 2. Federal Interagency Forum on Aging Related Statistics. Older Americans Key Indicators
778 of Well-Being. Information Dissemination Staff, National Center for Health Statistics,
779 3311 Toledo Road, Room 5412, Hyattsville, MD 20782. 2016. Available from:
780 https://agingstats.gov/docs/LatestReport/Older-Americans-2016-Key-Indicators-of-
781 WellBeing.pdf
782 3. He W, Goodkind D, Kowal P. An Aging World. U.S. Census Bureau, International
783 Population Reports, P95/16-1, U.S. Government Publishing Office, Washington, D.C.
784 2016. Available from:
785 https://www.census.gov/content/dam/Census/library/publications/2016/demo/p95-16-
786 1.pdf
787 4. Ezrati M. Aging demographics: A threat to the economy and finance. 2018. Available
788 from: https://www.forbes.com/sites/miltonezrati/2018/04/23/aging-demographics-a-
789 threat-to-the-economy-and-to-finance/#155cfa1e3f2e.
790 5. Acemoglu D. & Johnson S. Disease and development: The effect of life expectancy on
791 economic growth. National Bureau of Economic Research, Working Paper 12269 or
792 Journal of Political Economy. 2006; vol. 115 (6): 925 – 985. doi: 10.3386/w12269

6. Panda A, Arjona A, Sapey E, Bai F, Fikrig E, Montgomery RR, et al. Human innate immunosenescence: causes and consequences for immunity in old age. Trends in Immunology. 2009; 30 (7): 325 – 332. doi: 10.1016/j.it.2009.05
7. Nikolich-Žugich J. The twilight of immunity: emerging concepts in aging of the immune system. Nature Immunology. 2018; 19: 10 – 19. doi: 10.1038/s41590-017-0006-x
8. Graham P. Immunoscenescence comes of age, symposium on aging, research & immunity: the impact of genomics. EMBO Report. 2007; 8 (3): 220 – 223. doi: 10.1038/sj.embor.7400922
9. Weiskopf D, Weinberger B, Grubeck-Loebenstein B. Review: The aging of the immune system. Transplant International. 2009; 22: 1042-1050. doi: 10.1111/j.1432-2277.2009.00927.x
10. Aw D, Silva AB, Palmer DB. Immunosenescence: emerging challenges for an ageing population. Immunology. 2006; 120: 435 – 446. doi: 10.1111/j.1365-2567.2007.02555.x
11. Castle SC. Clinical relevance of age-related immune dysfunction. Clinical Infectious Diseases. 2000; 31: 578 - 585. doi: 1058-4838/2000/3102-0031.
12. Caruso C, Buffa S, Candore G, Colonna-Romano G, Dunn-Walters D, Kipling D, et al. Mechanisms of immunosenescence. Immunity & Aging. 2009; 6: 10. doi: 10.1186/1742-4933-6-10
13. Accardi G, Caruso C. Immune-inflammatory responses in the elderly: an update. Immunity & Aging. 2018; 5: 11. doi: 10.1186/s12979-018-0117-8
14. Accardi G, Caruso C. Immune-inflammatory responses in the elderly: an update. Immunity & Aging. 2018; 5: 11. doi: 10.1186/s12979-018-0117-8

15. Vallejo A. Immunological hurdles of ageing: Indispensable research of the human model. Ageing Res. Rev. 2011; 10 (3): 315 – 318 doi: 10.1016/j.arr.2011.01.005

16. Martorana A, Bulati M, Buffa S, Pellicano M, Caruso C, Candore G, et al. Immunosenescence, inflammation and Alzheimer's disease. Longev Healthspan. 2012; 1:8. doi: 10.1186/2046-2395-1-8

17. Weng N. Aging of the immune system: How much can the adaptive immune system adapt? Immunity. 2016; 24 (5): 495 – 499. doi: 10.1016/j.immuni.2006.05.001

18. McElhaney JE, Effros E. Immunosenescence: What does it mean to health outcomes in older adults? Current Opinion in Immunology. 2009; 21 (4): 418 – 424. doi: 10.1016/j.coi.2009.05.023

19. Onder G, Rezza G, Brusaferro S. Case-Fatality Rate and Characteristics of Patients Dying in Relation to COVID-19 in Italy. JAMA. 2020 May 12;323(18):1775-1776. doi: 10.1001/jama.2020.4683. Erratum in: JAMA. 2020 Apr 28;323(16):1619. PMID: 32203977.

20. Montecino-Rodrigues E, Berent-Maoz B, Dorshkind K. Causes, consequences and reversal of immune system aging. J. Clin. Invest. 2013; 123(3): 958–965. doi:10.1172/JCI64096.

21. Hayes L, Maue AC. Effects of aging on T-cell function. Current Opinion in Immunology. 2009; 21:414 -417. doi: 10.1016/j.coi.2009.05.009.

22. Pawelec G, Barnett Y, Forsey R, Frasca D, Globerson A, McLeod J, et al. T-cells and aging, January 2002 update. Front Biosci. 2002; 7:d1056-183. doi: 10.2741/A831

836 23. Jackola DR, Hallgren HM. Dynamic phenotypic restructuring of the CD4 and CD8 T-cell
837 subsets with age in healthy humans: a compartmental model analysis. Mech. Aging &
838 Dev. 1998; 105: 241–264. doi: 10.1016/S0047-6374(98)00089-X
839 24. Vibert J, Thomas-Vaslin V. Modelling T-cell proliferation: Dynamics heterogeneity
840 depending on cell differentiation, age, and genetic background.PLoS Comput Biol. 2017;
841 13(3):e1005417. doi: 10.1371/journal.pcbi.1005417
842 25. Thomas-Vaslin V, Six A, Pham HP, Dansokho C, Chaara W, Gouritin B, Bellier B,
843 Klatzmann D. Immunodepression and Immunosuppression During Aging,
844 Immunosuppression - Role in Health and Diseases. IntechOpen. 2012. DOI:
845 10.5772/29549.
846 26. Thomas-Vaslin V, Korthals Altes H, de Boer RJ, Klatzmann D. Comprehensive
847 Assessment and Mathematical Modeling of T Cell Population Dynamics and
848 Homeostasis. The Journal of Immunology. 2008; 180 (4) 2240-2250. DOI:
849 10.4049/jimmunol.180.4.2240
850 27. Vaz NM, Carvalho CR. On the origin of immunopathology. J Theor Biol. 2015 Jun
851 21;375:61-70. doi: 10.1016/j.jtbi.2014.06.006. Epub 2014 Jun 14. PMID: 24937801.
852 28. Southworth LK, Owen AB, Kim SK. Aging mice show a decreasing correlation of gene
853 expression within genetic modules. PLoS Genet. 2009; 5(12):e1000776. doi:
854 10.1371/journal.pgen.1000776
855 29. Viia-Vialaneix N, Liaubet L, Laurent T, Cherel P, Gamot A, SanCristobal M. The
856 structure of gene co-expression network reveals biological functions underlying eQTLs.
857 PLOS One. 2013; 8 (4): e60045. doi: 10.1371/journal.pone.0060045

30. Wisecaver JH, Borowsky AT, Tzin V, Jander G, Kliebenstein DJ, Rokas A. A Global Coexpression Network Approach for Connecting Genes to Specialized Metabolic Pathways in Plants. PlanT-cell. 2017;29(5):944-959. doi: 10.1105/tpc.17.00009

31. Monaco G, Van dam S, Casal Novo Ribeiro JL, Larbi A, De Magalhães JP. A comparison of human and mouse gene co-expression networks reveals conservation and divergence at the tissue, pathway and disease levels. BMC Evol Biol. 2015; 15:259. doi: 10.1186/s12862-015-0534-7

32. Gaiteri C, Ding Y, French B, Tseng GC, Sibille E. Review: Beyond modules and hubs – the potential of gene coexpression networks for investigating molecular mechanisms of complex brain disorders. Genes, Brain & Behavior. 2014; 13: 13 – 24. doi: 10.1111/gbb.12106

33. Pita-JuaÂrez Y, Altschuler G, Kariotis S, Wei W, Koler K, Green C, et al. The Pathway Coexpression Network: Revealing pathway relationships. PLoS Comput. Biol. 2018; 14(3): e1006042. doi: 10.1371/journal.pcbi.1006042

34. Simkó GI, Gyurkó D, Veres DV, Nánási T, Csermely P. Network strategies to understand the aging process and help age-related drug design. Genome Med. 2009; 1(9):90. doi: 10.1186/gm90

35. Witten TM. Introduction to the theory of aging networks. Interdiscip Top Gerontol. 2015; 40:1-17. doi: 10.1159/000364922

36. Witten TM, Bonchev D. Predicting aging/longevity-related genes in the nematode Caenorhabditis elegans. Chemistry & Diversity. 2007; 4: 2639 – 2655. doi: 10.1002/cbdv.200790216

880 37. Managbanag JR, Witten TM, Bonchev D, et al. Shortest-path network analysis is a useful
881 approach toward identifying genetic determinants of longevity. PLoS ONE. 2008;
882 3(11):e3802. doi: 10.1371/journal.pone.0003802
883 38. Ferrarini L, Bertelli L, Feala J, McCulloch AD, Paternostro G. A more efficient search
884 strategy for aging genes based upon connectivity. Bioinformatics. 2005; 21 (3): 338 –
885 348. doi: 10.1093/bioinformatics/bti004
886 39. Miraglia F, Vecchio F, Rossini PM. Physiological and pathological aging: a cortical
887 connectivity analysis by graph theory model applied to brain network. Clinical
888 Neurophysiology. 2015; Vol.126(1): pp.e2. doi: 10.1016/j.clinph.2014.10.026
889 40. Greer EL, Brunet A. Signaling networks in aging. J. Cell Sci. 2008; 121: 407 – 412. doi:
890 10.1242/jcs.021519
891 41. Budovsky A, Abramovich A, Cohen R, Chalifa-Caspi V, Fraifeld V. Longevity network:
892 Construction and implications. Mechanisms of Ageing and Development. 2007; 128: 117
893 – 124. doi: 10.1016/j.mad.2006.11.018
894 42. Kriete A, Lechner M, Clearfield D, Bohmann D. Computational systems biology of
895 aging. Systems Biology and Medicine. 2011; 3 (4): 414 – 428. doi: 10.1002/wsbm.126
896 43. Faisal FE, Milenkovi? T. Dynamic networks reveal key players in aging. Bioinformatics.
897 2014; 30(12):1721-9. doi: 10.1093/bioinformatics/btu089
898 44. Xue H, Xian B, Dong D, Xia K, Zhu S, Zhang Z, et al. A modular network model of
899 aging. Molecular Systems Biology. 2007; 3 (147). doi: 10.1038/msb4100189.
900 45. Leonov A, Titorenko VI. Critical Review: A network of interorganellar communications
901 underlies cellular aging. IUBMB Life. 2013; 65 (8): 665 – 674. doi: 10.1002/iub.1183

902 46. Petkov PM, Ding Y, Cassell MA, Zhang W, Wagner G, Sargent EE, et al. An efficient
903 SNP system for mouse genome scanning and elucidating strain relationships. Genome
904 Res. 2004; 14(9). Doi: 10.1101/gr.2825804
905 47. Albert R, DasGupta B, Hegde R, Sivanathan GS, Gitter A, Gursoy G, et al.
906 Computationally efficient measure of topological redundancy of biological and social
907 networks. Phys. Rev. E. 2011; 84: 036117. doi: 10.1103/PhysRevE.84.036117
908 48. Isakov N & Altman A. PKC-theta-mediated signal delivery from the TCR/CD28 surface
909 receptors. Front Immunol. 2012;3:273. doi: 10.3389/fimmu.2012.00273
910 49. Goronzy JJ, et al. Signaling pathways in aged T-cells – A reflection of T-cell
911 differentiation, cell senescence and host environment. Semin Immunol. 2012;24(5):365-
912 72. doi: 10.1016/j.smim.2012.04.003
913 50. Bavelas A. A mathematical model for group structures. Human Organization. 1948; 7:
914 16-30. doi: 10.17730/humo.7.3.f4033344851gl053
915 51. Bonchev D. Complexity analysis of yeast proteome network. Chemistry and Biodiversity.
916 2004; 1: 312 – 325. doi: 10.1002/cbdv.200490028
917 52. Ravasz E, Somera AL, Mongru DA, Oltavai ZN, Barabasi AL. Hierarchical organization
918 of modularity in metabolic networks. Science. 2002; 297: 1551 – 1555. doi:
919 10.1126/science.1073374
920 53. Lu X, Jain VV, Finn PW, Perkins, DL. Hubs in biological interaction networks exhibit
921 low changes in expression in experimental asthma. Molecular Systems Biology. 2007; 3.
922 doi: 10.1038/msb4100138.
923 54. Amaral LAN, Scala A, Barthelemy M, Stanley HE. Classes of behavior of small-world
924 networks. PNAS. 2000; 97 (21): 11149. doi: 10.1073/pnas.200327197

925 55. Li D, Li J, Ouyang S, Wang J, Wu S, Wan P, et al. Protein interaction networks of
926 Saccharomyces cerevisiae, Caenorhabditis elegans and Drosophila melanogaster: Large-
927 scale organization and robustness. Proteomics. 2006; 6: 456 – 461. doi:
928 10.1002/pmic.200500228
929 56. Rajarathinam T, Lin YH. Topological properties of protein-protein and metabolic
930 interaction networks of Drosophila melanogaster. Geno. Prot. Bioinfo. 2006; 4 (2): 80 –
931 89. doi: 10.1016/S1672-0229(06)60020-X
932 57. Jonsson PF, Bates PA. Global topological features of cancer proteins in the human
933 interactome. Bioinformatics. 2006; 22 (18):2291 – 2297 doi:
934 10.1093/bioinformatics/btl390.
935 58. Yu H, Kim PM, Sprecher E, Trifonov V, Gerstein M (2007) The importance of
936 bottlenecks in protein networks: Correlation with gene essentiality and expression
937 dynamics. PLoS Comput Biol 3(4): e59. doi: 10.1371/journal.pcbi.0030059
938 59. Scardoni G, Petterlini M, Laudanna C. Analyzing biological network parameters with
939 CentiScaPe. Bioinformatics. 2009; 25 (21): 2857 – 2859. doi:
940 10.1093/bioinformatics/btp517.
941 60. Qiao T, Shan W, Zhou C. How to identify the most powerful node in complex networks?
942 A novel entropy centrality approach. Entropy. 2017; 19: 614. doi: 10.3390/e19110614.
943 61. Albert, R. Scale-free networks in biology. J. Cell Sci. 2005; 118: 4948 – 4957. doi:
944 10.1242/jcs.02714
945 62. Keller EF. Revisiting “scale-free” networks. BioEssays. 2005; 27 (10): 1060 – 1068. doi:
946 10.1002/bies.20294

947 63. Wuchty S. Scale-free behavior in protein domain networks. Mol. Biol. Evol. 2001; 18
948 (9): 1694 – 1702. doi: 10.1093/oxfordjournals.molbev.a003957
949 64. Choromaski K, Matuszak M, MiKisz J. Scale-Free Graph with Preferential Attachment
950 and Evolving Internal Vertex Structure. Journal of Statistical Physics. 2013; 151 (6):
951 1175–1183. doi: 10.1007/s10955-013-0749-1
952 65. Fulop T, Dupuis G, Baehl S, Le Page A, Bourgade K, Frost E, et al. From inflamm-aging
953 to immune-paralysis: a slippery slope during aging for immune-adaptation.
954 Biogerontology. 2016; 17(1):147-57. doi: 10.1007/s10522-015-9615-7
955 66. Westera L, Van Hoeven V, Drylewicz J,Spierenburg G, van Velzen JF, de Boer RJ, et al.
956 Lymphocyte maintenance during healthy aging requires no substantial alterations in
957 cellular turnover. Aging Cell. 2015; 14(2):219-27. doi: 10.1111/acel.12311
958 67. Zhu J. T helper 2 (Th2) cell differentiation, type 2 innate lymphoid cell (ILC2)
959 development and regulation of interleukin-4 (IL-4) and IL-13 production. Cytokine.
960 2015; 75(1):14-24. doi: 10.1016/j.cyto.2015.05.010
961 68. Szklarczyk D, Franceschini A, Wyder S, Forslund K, Heller D, Huerta-Cepas J, et al.
962 STRING v10: protein-protein interaction networks, integrated over the tree of life.
963 Nucleic Acids Res. 2015;43:D447-52. doi: 10.1093/nar/gku1003
964 69. Revu S, Wu J, Henkel M, Rittenhouse N, Menk A, Delgoffe GM, et al. IL-23 and IL-1?
965 Drive Human Th17 Cell Differentiation and Metabolic Reprogramming in Absence of
966 CD28 Costimulation. Cell Rep. 2018; 22(10):2642-2653. doi:
967 10.1016/j.celrep.2018.02.044

968 70. Carlson MR, Zhang B, Fang Z, Mischel PS, Horvath S, Nelson SF. Gene connectivity,
969 function, and sequence conservation: predictions from modular yeast co-expression
970 networks. BMC Genomics. 2006; 7, 40. doi: 10.1186/1471-2164-7-40
971 71. De rosa V, Procaccini C, Calì G, Pirozzi G, Fontana S, Zappacosta S,et al. A key role of
972 leptin in the control of regulatory T-cell proliferation. Immunity. 2007; 26(2):241-55. doi:
973 10.1016/j.immuni.2007.01.011
974 72. Cipolletta D. Adipose tissue-resident regulatory T-cells: phenotypic specialization,
975 functions and therapeutic potential. Immunology. 2014; 142(4), 517-25. doi:
976 10.1111/imm.12262
977 73. Wang M, Windgassen D, Papoutsakis ET. Comparative analysis of transcriptional
978 profiling of CD3+, CD4+ and CD8+ T-cells identifies novel immune response players in
979 T-cell activation. BMC Genomics. 2008; 9:225. doi: 10.1186/1471-2164-9-225
980 74. Hale JS, Boursalian T, Turk G, Fink, P. Thymic output in aged mice. PNAS. 2006; 103
981 (22): 8447 – 8452. doi: 10.1073/pnas.0601040103
982 75. Weng NP, Araki Y, Subedi K. The molecular basis of the memory T-cell response:
983 differential gene expression and its epigenetic regulation. Nature Reviews Immunology.
984 2012; 12(4), 306-15. doi: 10.1038/nri3173.
985 76. Taylor J, Reynolds L, Hou L, Lohman K, Cui W, Kritchevsky S, et al. Transcriptomic
986 profiles of aging in naïve and memory CD4+ cells from mice. Immunity & ageing. 2017;
987 14, 15. doi:10.1186/s12979-017-0092-5.
988 77. Rane S, Hogan T, Seddon B, Yates AJ. Age is not just a number: Naive T-cells increase
989 their ability to persist in the circulation over time. PLoS Biol. 2018; 16(4):e2003949. doi:
990 10.1371/journal.pbio.2003949

78. Almeida L, Lochner M, Berod L, Sparwasser T. Metabolic pathways in T-cell activation and lineage differentiation. Semin Immunol. 2016; 28(5):514-524. doi: 10.1016/j.smim.2016.10.009

79. Hudgins AD, Tazearslan C, Tare A, Zhu Y, Huffman D, Suh Y. Age- and Tissue-Specific Expression of Senescence Biomarkers in Mice. Frontiers in Genetics. 2018; 9, 59. doi: 10.3389/fgene.2018.00059.

Supporting Information

S1 Table. Summary of genes appearing in the age-related GCNs. Genes with co-expression relationships represented in either or both the old and young networks along with their human ortholog and known functions.

S2 Table. Network of 2-month old mouse CD3+ splenocytes. All co-expression relationships appearing in the 2-month old mouse GCN are documented in this file.

S3 Table. Network of 22/24-month old mouse CD3+ splenocytes. All co-expression relationships appearing in the 22/24-month old mouse GCN are documented in this file.

S1 Fig. Heatmap representation of gene expression signature from splenic T-cells obtained from young and old mice and across 3 mouse strains. The C2-5 signature with 130 selected genes was identified from ICA/GSEA. The C2-5 signature distinguishes young from old mice (A), but also the genetic origins in young mice (B). The clustering of the 3 strains in young mice (B) is, however, lost in old mice (C). Key genes where co-expression was observed are underlined with TCR related genes (green boxes) co-stimulation molecules as CD28 (pink), CD69 an early

activation marker and other markers revealed as centrality as the receptor for leptin (Leprotl1 gene).

S2 Fig. Ingenuity Pathway Analysis of the C2-5 aging signature reveal altered gene expression and pathways in old mice. (signature score: 40, focus molecules: 23). In A) genes with altered expression in the T-cells from old mice are involved in cellular development, cellular growth and proliferation, hematological system development and function. Genes belonging to TCR complex are underlined in green, CD28 downstream genes in orange, and those involved in T-cell signal transduction in blue. B) For this C2-5 aging signature, the top disease and functions are indicated.

S3 Fig. MCODE generated network clusters. In this figure we display only the MCODE generated clusters, not the full network structures. A total of four clusters were generated for the young group (A), and six clusters generated for the old group (B).

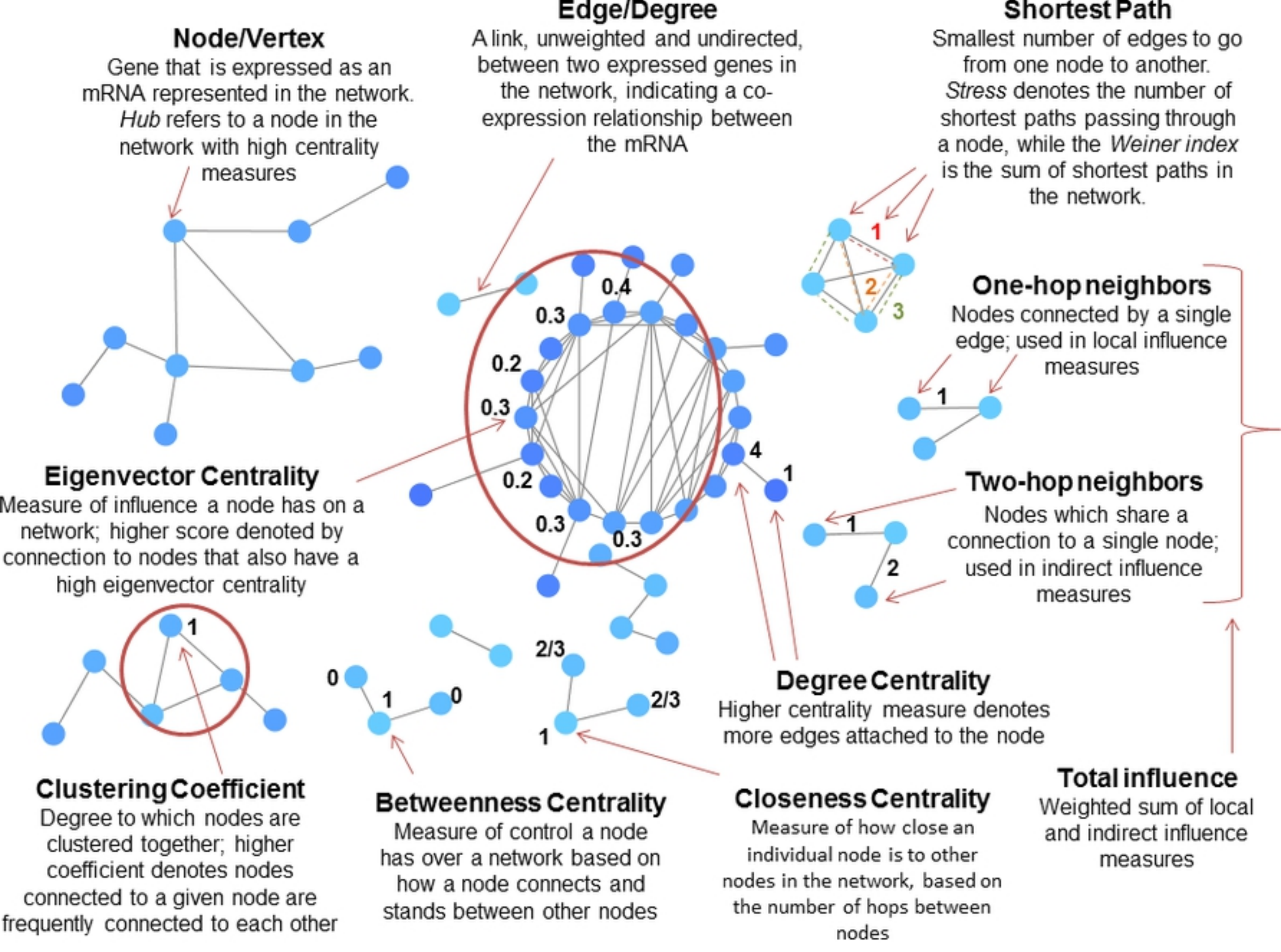
Node/Vertex
Gene that is expressed as an mRNA represented in the network. *Hub* refers to a node in the network with high centrality measures
Edge/Degree
A link, unweighted and undirected, between two expressed genes in the network, indicating a co-expression relationship between the mRNA
Shortest Path
Smallest number of edges to go from one node to another. *Stress* denotes the number of shortest paths passing through a node, while the *Weiner index* is the sum of shortest paths in the network.
1
2
3
One-hop neighbors
Nodes connected by a single edge; used in local influence measures
1
Two-hop neighbors
Nodes which share a connection to a single node; used in indirect influence measures
1
2
Eigenvector Centrality
Measure of influence a node has on a network; higher score denoted by connection to nodes that also have a high eigenvector centrality
0.4
0.3
0.2
0.3
0.2
0.3
0.3
4
1
1
Clustering Coefficient
Degree to which nodes are clustered together; higher coefficient denotes nodes connected to a given node are frequently connected to each other
0
1
0
2/3
1
2/3
Betweenness Centrality
Measure of control a node has over a network based on how a node connects and stands between other nodes
Degree Centrality
Higher centrality measure denotes more edges attached to the node
Closeness Centrality
Measure of how close an individual node is to other nodes in the network, based on the number of hops between nodes
Total influence
Weighted sum of local and indirect influence measures

Figure1

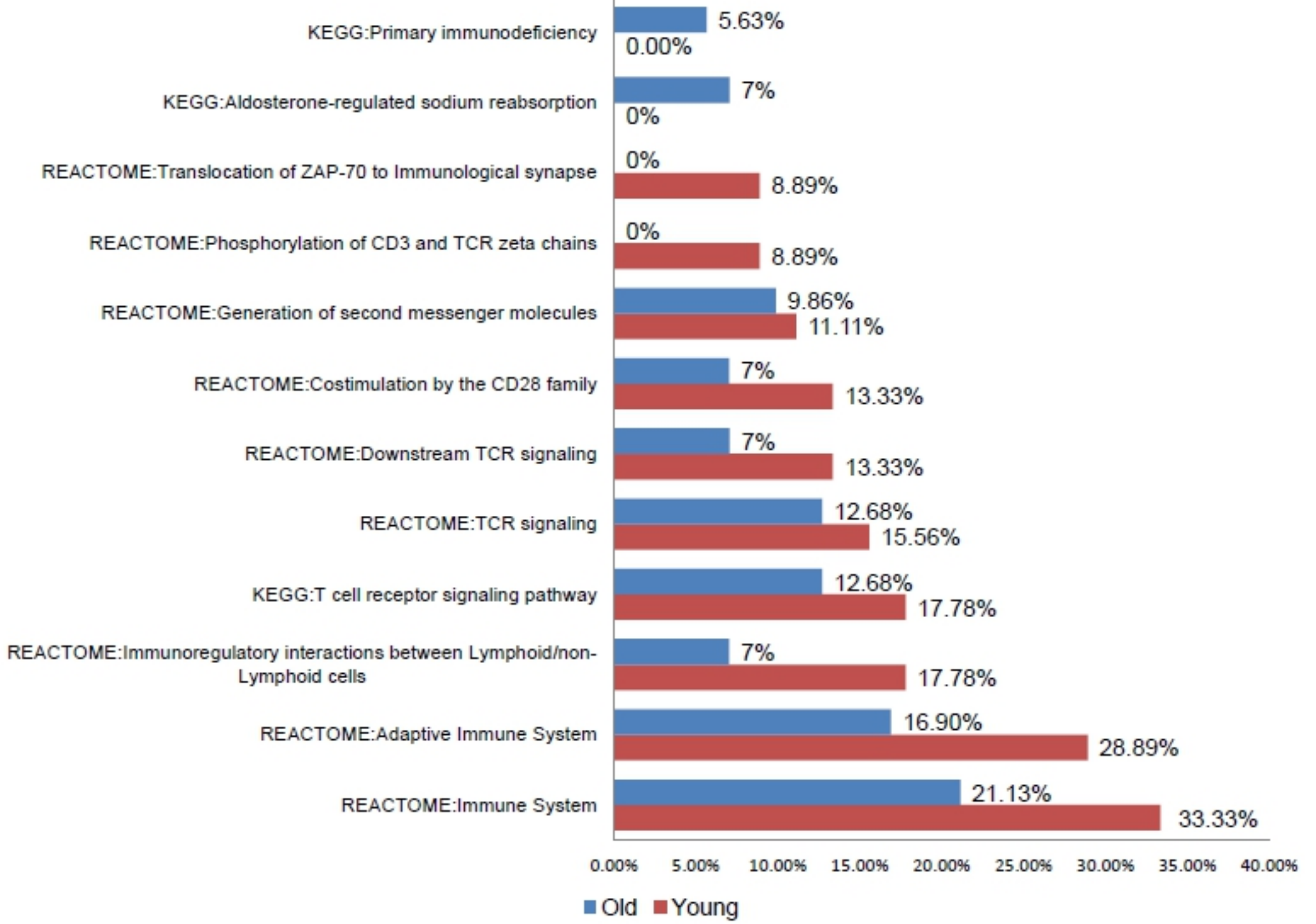
KEGG:Primary immunodeficiency
5.63%
0.00%
KEGG:Aldosterone-regulated sodium reabsorption
7%
0%
REACTOME:Translocation of ZAP-70 to Immunological synapse
0%
8.89%
REACTOME:Phosphorylation of CD3 and TCR zeta chains
0%
8.89%
REACTOME:Generation of second messenger molecules
9.86%
11.11%
REACTOME:Costimulation by the CD28 family
7%
13.33%
REACTOME:Downstream TCR signaling
7%
13.33%
REACTOME:TCR signaling
12.68%
15.56%
KEGG:T cell receptor signaling pathway
12.68%
17.78%
REACTOME:Immunoregulatory interactions between Lymphoid/non-Lymphoid cells
7%
17.78%
REACTOME:Adaptive Immune System
16.90%
28.89%
REACTOME:Immune System
21.13%
33.33%
0.00% 5.00% 10.00% 15.00% 20.00% 25.00% 30.00% 35.00% 40.00%
Old
Young

Figure2

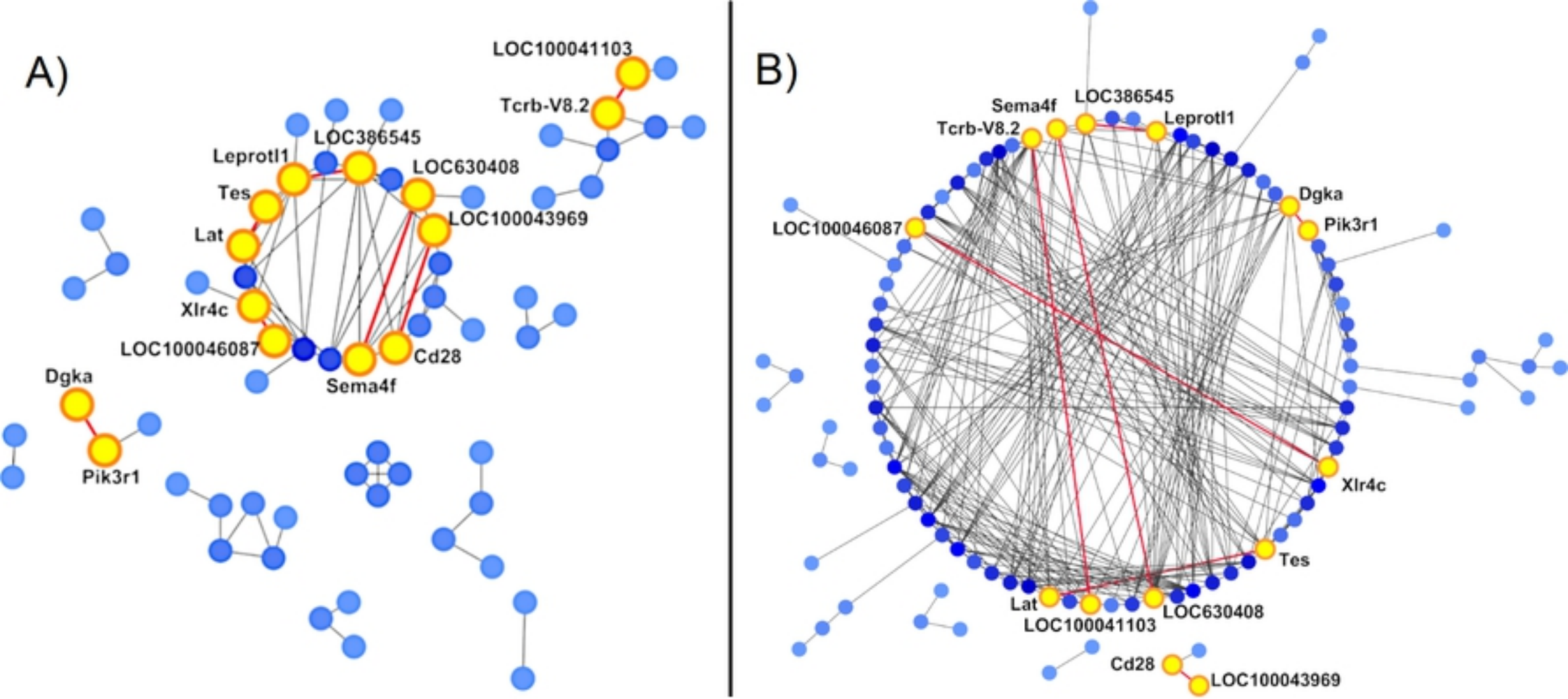
A)
LOC100041103
Tcrb-V8.2
LOC386545
Leprotl1
LOC630408
Tes
LOC100043969
Lat
Xlr4c
LOC100046087
Cd28
Sema4f
Dgka
Pik3r1
B)
Sema4f
LOC386545
Tcrb-V8.2
Leprotl1
Dgka
LOC100046087
Pik3r1
Xlr4c
Tes
Lat
LOC630408
LOC100041103
Cd28
LOC100043969

Figure3

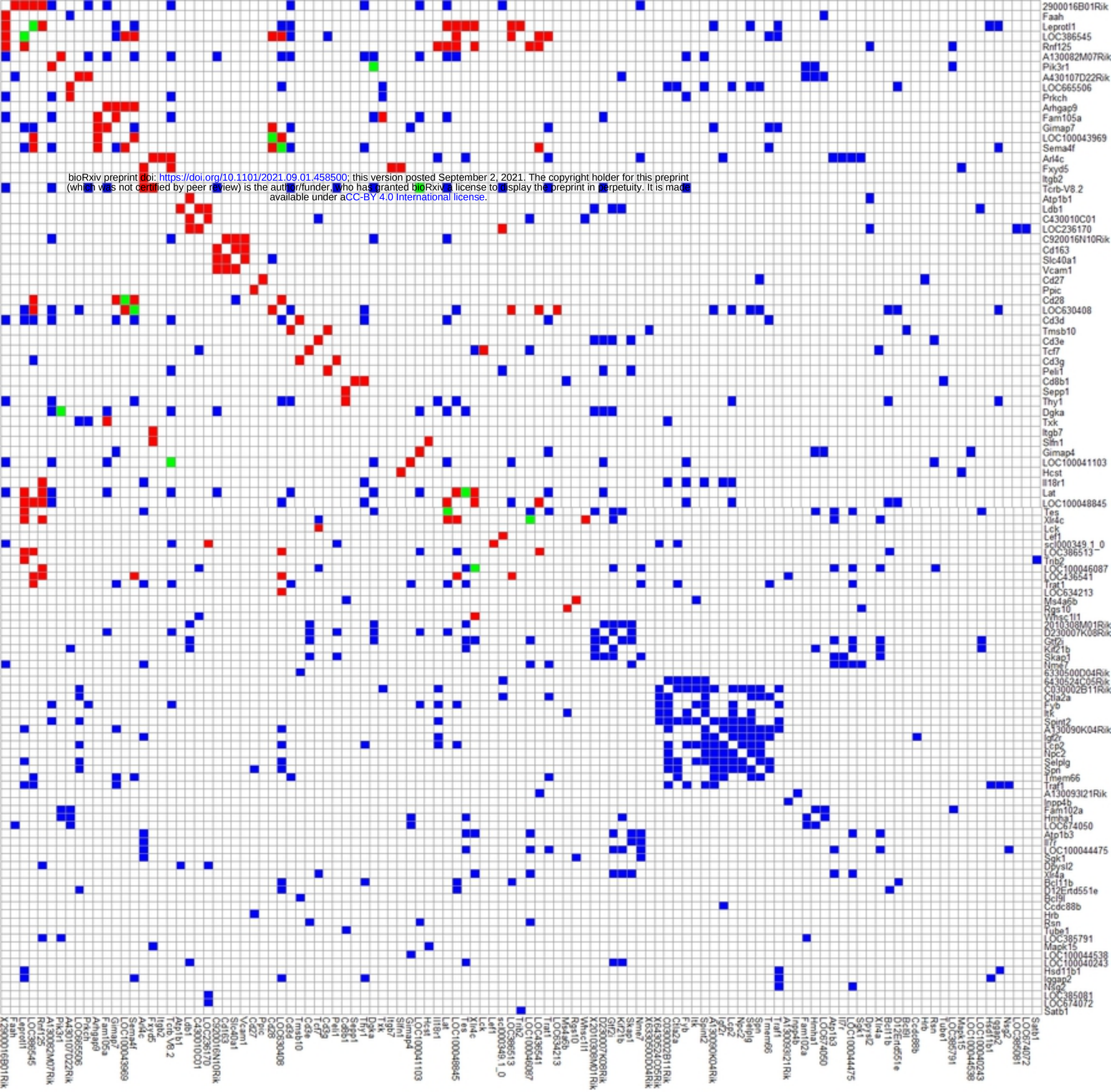

Figure4

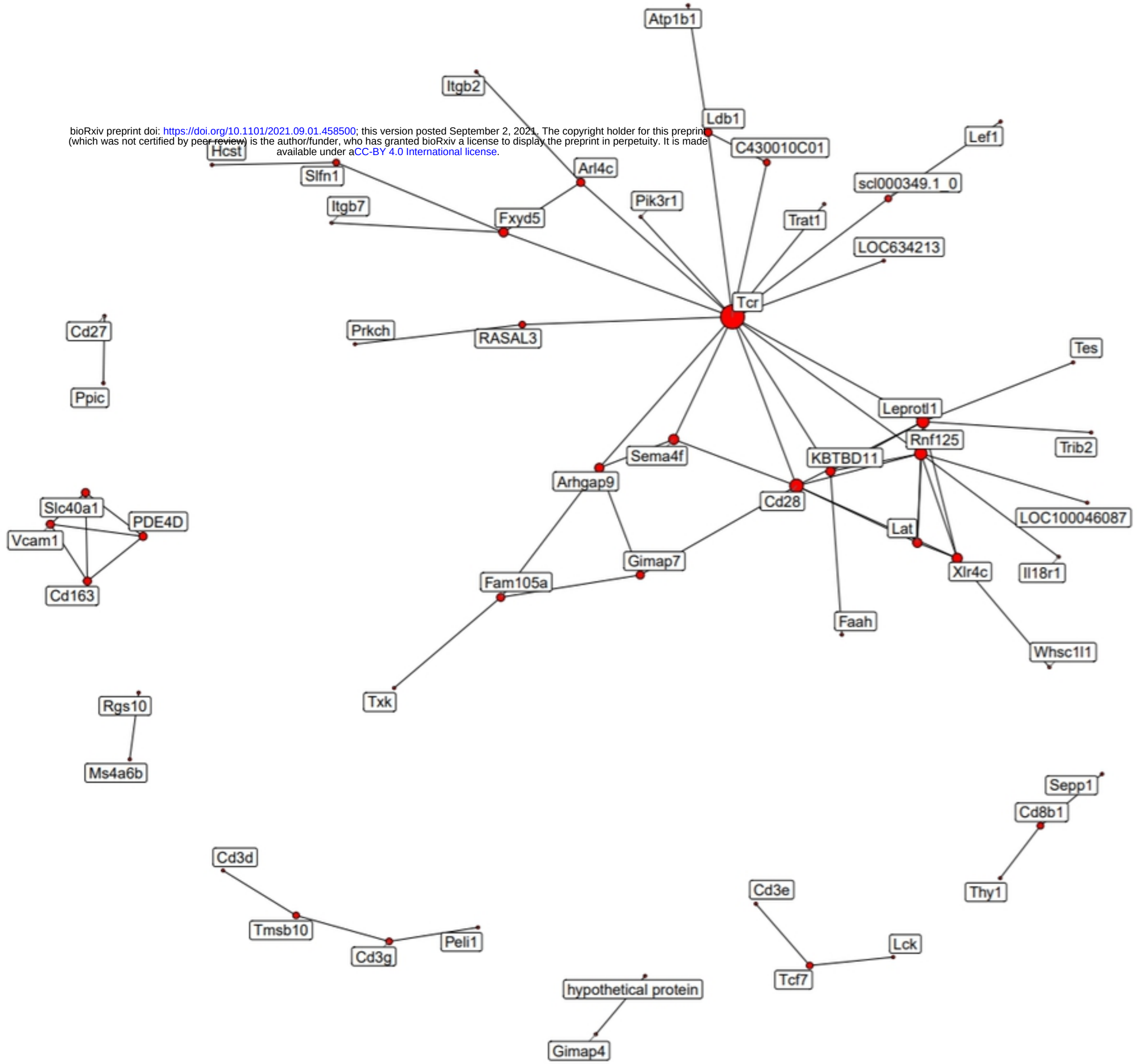

Figure5

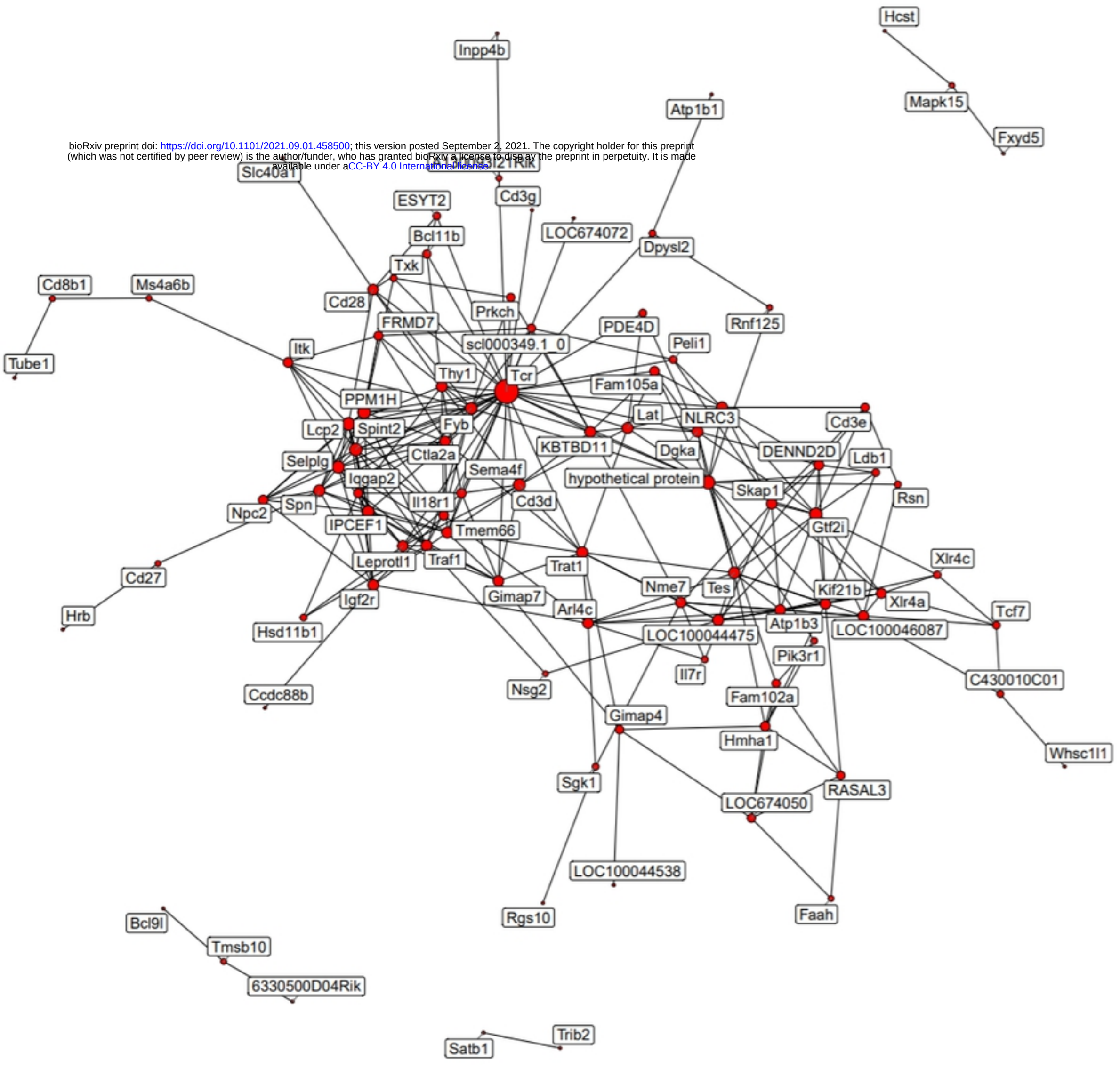

Figure6

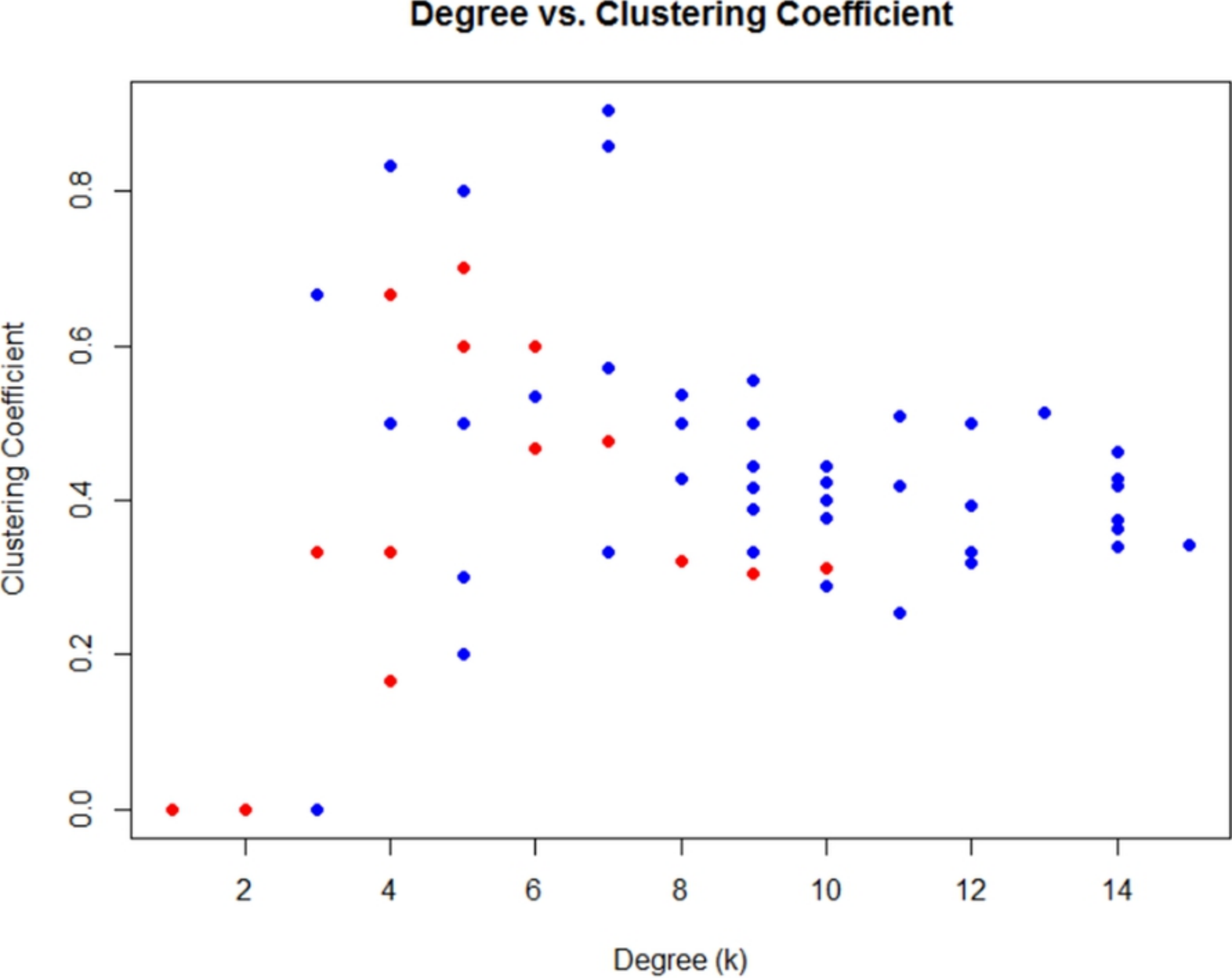
Degree vs. Clustering Coefficient
Clustering Coefficient
0.0
0.2
0.4
0.6
0.8
2
4
6
8
10
12
14
Degree (k)

Figure7

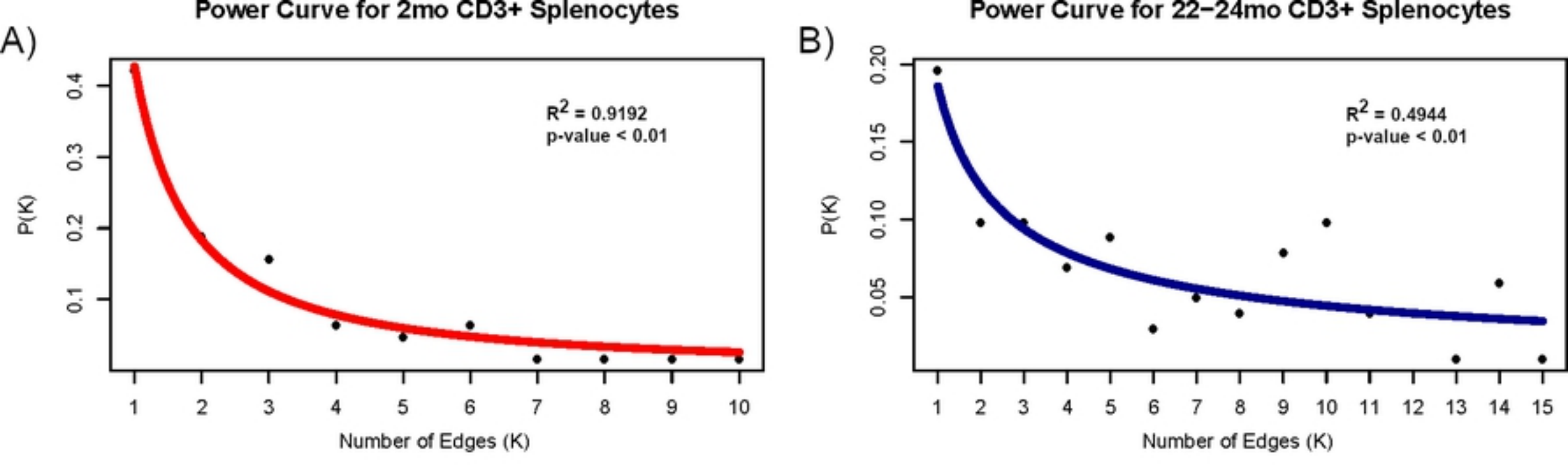
A)
Power Curve for 2mo CD3+ Splenocytes
R^2 = 0.9192
p-value < 0.01
P(K)
0.1
0.2
0.3
0.4
1
2
3
4
5
6
7
8
9
10
Number of Edges (K)
B)
Power Curve for 22−24mo CD3+ Splenocytes
R^2 = 0.4944
p-value < 0.01
P(K)
0.05
0.10
0.15
0.20
1
2
3
4
5
6
7
8
9
10
11
12
13
14
15
Number of Edges (K)

Figure8